On the Required Number of Antennas in a Point-to-Point Large-but-Finite MIMO System: Outage-Limited Scenario

On the Required Number of Antennas in a Point-to-Point Large-but-Finite MIMO System: Outage-Limited Scenario

Behrooz Makki, Tommy Svensson, Thomas Eriksson and Mohamed-Slim Alouini, *Fellow, IEEE*

***Abstract*—This paper investigates the performance of the point-to-point multiple-input-multiple-output (MIMO) systems in the presence of a large but finite numbers of antennas at the transmitters and/or receivers. Considering the cases with and without hybrid automatic repeat request (HARQ) feedback, we determine the minimum numbers of the transmit/receive antennas which are required to satisfy different outage probability constraints. Our results are obtained for different fading conditions and the effect of the power amplifiers efficiency/feedback error probability on the performance of the MIMO-HARQ systems is analyzed. Then, we use some recent results on the achievable rates of finite block-length codes, to analyze the effect of the codewords lengths on the system performance. Moreover, we derive closed-form expressions for the asymptotic performance of the MIMO-HARQ systems when the number of antennas increases. Our analytical and numerical results show that different outage requirements can be satisfied with relatively few transmit/receive antennas.**

I. Introduction

The next generation of wireless networks must provide data streams for everyone everywhere at any time. Particularly, the data rates should be orders of magnitude higher than those in the current systems; a demand that creates serious power concerns because the data rate scales with power monotonically. The problem becomes even more important when we remember that currently the wireless network contributes $\sim 2\%$ of global CO_2 emissions and its energy consumption is expected to increase $16-20\%$ every year [1].

To address the demands, the main strategy persuaded in the last few years is the network *densification* [2]. One of the promising techniques to densify the network is to use many antennas at the transmit and/or receive terminals. This approach is referred to as massive or large multiple-input-multiple-output (MIMO) in the literature.

In general, the more antennas the transmitter and/or the receiver are equipped with, the better the data rate/link reliability. Particularly, the capacity increases and the required uplink/downlink transmit power decreases with the number of antennas. Thus, the trend is towards asymptotically high number of antennas. This is specially because millimeter wave communication [3], [4], which is indeed expected to be implemented in the next generation of wireless networks, makes it possible to assemble many antennas at the transmit/receive terminals. However, large MIMO implies challenges such as hardware impairments and signal processing complexity which may limit the number of antennas in practice. Also, one of the main bottlenecks of large MIMO is the channel state information (CSI) acquisition, specifically at the transmitter. Therefore, it is interesting to use efficient feedback schemes such as hybrid automatic repeat request (HARQ) whose feedback overhead does not scale with the number of antennas.

The performance of HARQ protocols in single-input-single-output (SISO) and MIMO systems is studied in, e.g., [5]–[8] and [9]–[20], respectively. MIMO transmission with many antennas is advocated in [21], [22] where the time-division duplex (TDD)-based training is utilized for CSI feedback[1]. Also, [23]–[29] introduce TDD-based schemes for large systems. Particularly, [29] studies the required number of antennas in TDD-based multi-cellular systems with pilot contamination being the major issue. Here, different precoders are designed such that the network sum throughput is optimized. In the meantime, frequency division duplex (FDD)-based massive MIMO has recently attracted attentions and low-overhead CSI acquisition methods were proposed [30]–[32]. Considering imperfect CSI, [33] derives lower bounds for the uplink achievable rate of the MIMO setups with large but finite number of antennas. Then, [34] (resp. [35]) studies the zero-forcing based TDD (resp. TDD/FDD) systems under the assumption that the number of transmit antennas and the single-antenna users are asymptotically large while their ratio remains bounded. Finally, [39] derives approximate expressions for the mutual information of MIMO systems with large number of transmit and/or receive antennas, and evaluates the effect of quantized feedback/scheduling on the system performance (For detailed review of the literature on massive MIMO, see [36]–[38]).

To summarize, a large part of the literature on the point-to-point and multi-user large MIMO is based on the assumption of asymptotically many antennas. Then, a natural question is how many transmit/receive antennas do we require in practice to satisfy different quality-of-service requirements. The interesting answer this paper establishes is relatively few, for a large range of outage probabilities. Moreover, the results

Behrooz Makki, Tommy Svensson and Thomas Eriksson are with Chalmers University of Technology, Gothenburg, Sweden, Email: {behrooz.makki, tommy.svensson, thomase}@chalmers.se. Mohamed-Slim Alouini is with the King Abdullah University of Science and Technology (KAUST), Thuwal, Makkah Province, Saudi Arabia, Email: slim.alouini@kaust.edu.sa

Part of this work has been accepted for presentation at the IEEE ICUWB 2015.

The research leading to these results received funding from the European Commission H2020 programme under grant agreement $n^\circ 671650$ (5G PPP mmMAGIC project), and from the Swedish Governmental Agency for Innovation Systems (VINNOVA) within the VINN Excellence Center Chase.

[1]The results of [21]–[38] are mostly on multi-user MIMO networks, as opposed to our work on point-to-point systems. However, because many of the analytical results in [21]–[38] are applicable in point-to-point systems as well, these works are cited.

of [5]–[39] are mainly obtained under the assumption that the instantaneous achievable rate of a user is given by $\log(1+x)$ with x standing for the user's instantaneous received signal-to-interference-and-noise ratio (SINR). This is an appropriate assumption in the cases with long codewords. However, it is also interesting to analyze the system performance in the cases with codewords of finite length where $\log(1+x)$ is not an appropriate approximation for the achievable rates.

Here, we study the outage-limited performance of point-to-point MIMO systems in the cases with large but finite number of antennas. Using the fundamental results of [39] on the mutual information of MIMO setups, we derive closed-form expressions for the required number of transmit and/or receive antennas satisfying various outage probability requirements (Theorem 1). The results are obtained for different fading conditions and in the cases with or without HARQ. Furthermore, we analyze the effect of the power amplifiers (PAs) efficiency (Section IV.A), erroneous feedback (Section IV.C) and spatial/temporal correlations (Sections V.B, V.C) on the system performance and study the outage probability in the cases with adaptive power allocation between the HARQ retransmissions (Theorem 3). Then, we use the recent results of [40], [41] on the achievable rates of finite block-length codes to analyze the outage probability in the cases with short packets and erroneous feedback (Section IV.C). Finally, we study the asymptotic performance of MIMO systems. Particularly, denoting the outage probability and the number of transmit and receive antennas by $\Pr(\text{Outage}), N_{\text{t}}$ and N_{r}, respectively, we derive closed-form expressions for the normalized outage factor which is defined as $\Gamma = -\frac{\log(\Pr(\text{Outage}))}{N_{\text{t}}N_{\text{r}}}$ when the number of transmit and/or receive antennas increases (Theorem 2).

As opposed to [5]–[20], we consider large MIMO setups and determine the required number of antennas in outage-limited conditions. Also, the paper is different from [21]–[39] because we study the outage-limited scenarios in point-to-point systems, implement HARQ and the number of antennas is considered to be finite. The differences in the problem formulation and the channel model makes the problem solved in this paper completely different from the ones in [5]–[39], leading to different analytical/numerical results, as well as to different conclusions. Finally, our discussions on the asymptotic outage performance of the MIMO setups, finite block-length analysis and the effect of PAs on the performance of MIMO-HARQ schemes have not been presented before.

Our analytical and numerical results indicate that:

- Different quality-of-service requirements can be satisfied with relatively few transmit/receive antennas. For instance, consider a SIMO (S: single) setup without HARQ and transmission signal-to-noise ratio (SNR) 5 dB. Then, with the data rate of 3 nats-per-channel use (npcu), the outage probabilities 10^{-3}, 10^{-4} and 10^{-5} are guaranteed with 16, 18 and 20 receive antennas, respectively (Fig. 5a). Also, the implementation of HARQ reduces the required number of antennas significantly (Fig. 3).
- At moderate/high SNRs, the required number of transmit (resp. receive) antennas scales with $(Q^{-1}(\theta))^2$, $\frac{1}{MT}$, and $\frac{1}{(\log(\phi))^2}$ linearly, if the number of receive (resp. transmit) antennas is fixed. Here, M is the maximum number of HARQ retransmission rounds, T is the number of channel realizations experienced in each round, ϕ denotes the SNR, θ is the outage probability constraint and $Q^{-1}(.)$ represents the inverse Gaussian Q-function. These scaling laws are changed drastically, if the numbers of the transmit and receive antennas are adapted simultaneously (see Theorem 1 and its following discussions for details).
- For different fading conditions, the normalized outage factor $\Gamma = -\frac{\log(\Pr(\text{Outage}))}{N_{\text{t}}N_{\text{r}}}$ converges to constant values, unless the number of receive antennas grows large while the number of transmit antennas is fixed (see Theorem 2). Also, for every given number of transmit/receive antennas, the normalized outage factor increases with MT linearly.
- There are mappings between the performance of MIMO-HARQ systems in quasi-static, slow- and fast-fading conditions, in the sense that with proper scaling of the channel parameters the same outage probability is achieved in these conditions. This point provides an appropriate connection between the papers considering one of these fading models.
- Adaptive power allocation between the HARQ retransmissions leads to marginal antenna requirement reduction, while the system performance is remarkably affected by the inefficiency of the PAs. Also, the spatial correlation between the antennas increases the required number of antennas while, for a large range of correlation conditions, the same scaling rules hold for the uncorrelated and correlated fading scenarios.
- Finally, with low number of antennas the system performance is considerably affected by the feedback error probability. However, the effect of erroneous feedback decreases with the number of antennas. Moreover, for a given number of nats per codeword, increasing the number of antennas can effectively reduce the required codeword length leading to low data transmission delay.

Notations. In the following, we denote the determinant, the Hermitian and the (i,j)-th element of the matrix $\mathbf{X}$ by $|\mathbf{X}|$, $\mathbf{X}^{\text{h}}$ and $\mathbf{X}[i,j]$, respectively. Also, $E[\cdot]$ is the expectation operator, $\bigotimes$ denotes the Kronecker product and $Q(x) = \frac{1}{\sqrt{2\pi}}\int_x^\infty e^{-\frac{u^2}{2}}\mathrm{d}u$ is the Gaussian Q-function. Then, $\lceil x \rceil$ denotes the smallest integer number larger than or equal to x, and the $\arg$ function is used to indicate the solution of an equation. Finally, $Q^{-1}(\cdot)$ and $W(\cdot)$ represent the inverse Q-function and the Lambert W function, respectively.

II. System Model

Table 1 summarizes the set of parameters used throughout the paper. We consider a point-to-point MIMO setup with N_{t} transmit antennas and N_{r} receive antennas. We study the block-fading conditions where the channel coefficients remain constant during the channel coherence time and then change to other values based on their probability density function (PDF). In this way, the received signal is given by

$$\mathbf{Y} = \mathbf{H}\mathbf{X} + \mathbf{Z}, \mathbf{Z} \in \mathcal{C}^{N_{\text{r}}\times 1}, \tag{1}$$

where $\mathbf{H} \in \mathcal{C}^{N_{\text{r}}\times N_{\text{t}}}$ is the fading matrix, $\mathbf{X} \in \mathcal{C}^{N_{\text{t}}\times 1}$ is the transmitted signal and $\mathbf{Z} \in \mathcal{C}^{N_{\text{r}}\times 1}$ denotes the independent and

Table I
THE DEFINITION OF PARAMETERS.

Parameter	Definition	Parameter	Definition
Γ	Normalized outage factor	ϕ	Transmission power
$N_{\rm t}$	Number of transmit antennas	μ	Mean of a random variable
$N_{\rm r}$	Number of receive antennas	σ^2	Variance of a random variable
M	Maximum number of HARQ retransmissions	$\phi^{\max}$	Maximum output power
T	Number of channel realizations in each round	$\phi^{\rm cons}$	Consumed power
θ	Outage probability constraint	L	Sub-codewords length
q	Nats per codeword	β	Spatial correlation parameter
R	Initial transmission rate	ϑ	Power amplifier parameter
ϵ	Maximum efficiency of power amplifier	ν	Temporal correlation parameter

identically distributed (IID) complex Gaussian noise matrix. Such a setup is of interest in, e.g., side-to-side communication between vehicles/buildings/lamp posts [42], as well as in wireless backhaul point-to-point links where the trend is to introduce MIMO and thereby achieving multiple parallel streams, e.g., [43]. The results are mainly given for IID Rayleigh-fading channels where each element of the channel matrix $\mathbf{H}$ follows a complex Gaussian distribution $\mathcal{CN}(0,1)$ (To analyze the effect of the antennas spatial correlation, see Fig. 9 and Section V.B). The channel coefficients are initially assumed to be known by the receiver. Taking the block-fading condition into account, this is an appropriate assumption in outage-constrained point-to-point MIMO setups with long codewords where sufficiently large number of pilot signals can be used to provide the receiver with accurate channel estimation [5]–[20]. Then, in Section IV.C, we study the other extreme case with codewords of finite length and no CSI at the receiver. On the other hand, there is no CSI available at the transmitter except the HARQ feedback bits (see [44] for mappings between the performance of the systems using HARQ and joint HARQ and quantized CSI feedback). The feedback channel is initially supposed to be error-free, while we study the cases with erroneous feedback in Section IV.C.

As the most promising HARQ approach leading to highest throughput/lowest outage probability [5], [6], [9], [14], we consider the incremental redundancy (INR) HARQ with a maximum of M retransmissions, i.e., the message is retransmitted a maximum of M times. Note that setting $M=1$ represents the cases without HARQ, i.e., open-loop communication. Also, a packet is defined as the transmission of a codeword along with all its possible retransmissions. We investigate the system performance for three different fading conditions:

- **Fast-fading**. Here, it is assumed that a finite number of channel realizations are experienced within each HARQ retransmission round.
- **Slow-fading**. In this model, the channel is supposed to change between two successive retransmission rounds, while it is fixed for the duration of each retransmission.
- **Quasi-static**. The channel is assumed to remain fixed within a packet period.

Fast-fading is an appropriate model for fast-moving users or users with long codewords compared to the channel coherence time [14], [45]. On the other hand, slow-fading can properly model the cases with users of moderate speeds or frequency-hopping schemes [10]–[12]. Finally, the quasi-static represents the scenarios with slow-moving or stationary users, e.g., [5], [9], [17]–[20].

III. PROBLEM FORMULATION

Considering the INR HARQ with a maximum of M retransmissions, q information nats are encoded into a *parent* codeword of length ML channel uses and the codeword is divided into M sub-codewords of length L. In each retransmission round, the transmitter sends a new sub-codeword and the receiver combines all signals received up to the end of that round. Thus, the equivalent rate at the end of round m is $\frac{q}{mL}=\frac{R}{m}$ npcu where R denotes the initial transmission rate. The retransmissions continue until the message is correctly decoded by the receiver or the maximum permitted retransmission round is reached.

Assuming fast-fading conditions with T independent fading realizations $\mathbf{H}((m-1)T+1),\ldots,\mathbf{H}(mT)$ in the mth round and an isotropic Gaussian input distribution over all transmit antennas, the results of, e.g., [46, Chapter 15], [47, Chapter 7], can be used to find the outage probability of the INR-based MIMO-HARQ scheme as

$$\Pr(\text{Outage})^{\text{Fast-fading}} = \Pr\left(\frac{1}{MT}\sum_{n=1}^{M}\sum_{t=(n-1)T+1}^{nT}\log\left|\mathbf{I}_{N_{\rm r}}+\frac{\phi}{N_{\rm t}}\mathbf{H}(t)\mathbf{H}(t)^h\right|\le\frac{R}{M}\right). \tag{2}$$

Here, ϕ (in dB, $10\log_{10}\phi$) is the total transmission power and $\frac{\phi}{N_{\rm t}}$ is the transmission power per transmit antenna (because the noise variance is set to 1, ϕ represents the SNR as well). Also, $\mathbf{I}_{N_{\rm r}}$ represents the $N_{\rm r}\times N_{\rm r}$ identity matrix.

Considering $T=1$ in (2), the outage probability is rephrased as

$$\Pr(\text{Outage})^{\text{Slow-fading}} = \Pr\left(\frac{1}{M}\sum_{n=1}^{M}\log\left|\mathbf{I}_{N_{\rm r}}+\frac{\phi}{N_{\rm t}}\mathbf{H}(n)\mathbf{H}(n)^h\right|\le\frac{R}{M}\right), \tag{3}$$

in a slow-fading channel. Also, setting $\mathbf{H}(t)=\mathbf{H},\forall t=1,\ldots,MT$, the outage probability in a quasi-static fading channel is given by

$$\Pr(\text{Outage})^{\text{Quasi-static}} = \Pr\left(\log\left|\mathbf{I}_{N_{\rm r}}+\frac{\phi}{N_{\rm t}}\mathbf{H}\mathbf{H}^h\right|\le\frac{R}{M}\right). \tag{4}$$

Using (2)-(4) for given initial transmission rate and SNR, the problem formulation of the paper can be expressed as

$$\{\hat{N}_{\rm t},\hat{N}_{\rm r}\}=\underset{N_{\rm t},N_{\rm r}}{\arg\min}\{\Pr(\text{Outage})\le\theta\}. \tag{5}$$

Here, θ denotes an outage probability constraint and $\hat{N}_{\rm t},\hat{N}_{\rm r}$ are the minimum numbers of transmit/receive antennas that

are required to satisfy the outage probability constraint. In the following, we solve (5) in the cases where one of the transmit or receive antennas is given, or there is a relationship between the number of transmit and receive antennas. Particularly, we study (5) in four distinct cases:

- Case 1: $N_{\rm r}$ is large but $N_{\rm t}$ is given.
- Case 2: $N_{\rm r}$ is given but $N_{\rm t}$ is large.
- Case 3: Both $N_{\rm t}$ and $N_{\rm r}$ are large and the transmission SNR is low.
- Case 4: Both $N_{\rm t}$ and $N_{\rm r}$ are large and the transmission SNR is high.

It is worth noting that the three first cases are commonly of interest in large MIMO systems. However, for the completeness of the discussions, we consider Case 4 as well. Moreover, in harmony with the literature [34], [35][2], we analyze Cases 3-4 under the assumption

$$\frac{N_{\rm t}}{N_{\rm r}} = K, \tag{6}$$

with K being a constant. However, as seen in the following, it is straightforward to extend the results of the paper to the cases with other relations between the numbers of antennas.

The basis of our analyses comes from the well-established results of [39] which approximate the instantaneous mutual information of MIMO setups by equivalent Gaussian variables. Then, we use the results to derive the minimum number of transmit/receive antennas in outage-constrained conditions (Theorem 1), define and analyze the normalized outage factor (Theorem 2), study the effect of imperfect power amplifiers (Section IV.A), derive outage-optimized power allocation between the HARQ retransmissions (Theorem 3), and perform finite block-length analysis of MIMO-HARQ systems with erroneous feedback (Section IV.C).

Finally, we should mention that, as (5) is a non-convex problem, there is no guarantee that the globally optimal parameters are determined by any method, except exhaustive search algorithms. However, as we show in Section V, our approximation schemes lead to very close results to the ones obtained by exhaustive search.

IV. Performance Analysis

To solve (5), let us first introduce Lemma 1. The lemma is of interest because it represents the outage probability as a function of the number of antennas, and simplifies the performance analysis remarkably.

Lemma 1: Considering Cases 1-4, the outage probability of the INR-based MIMO-HARQ system is given by

$$\begin{cases} \Pr(\text{Outage})^{\text{Fast-fading}} = Q\left(\frac{\sqrt{MT}(\mu-\frac{R}{M})}{\sigma}\right), & \text{(i)} \\ \Pr(\text{Outage})^{\text{Slow-fading}} = Q\left(\frac{\sqrt{M}(\mu-\frac{R}{M})}{\sigma}\right), & \text{(ii)} \\ \Pr(\text{Outage})^{\text{Quasi-static}} = Q\left(\frac{\mu-\frac{R}{M}}{\sigma}\right), & \text{(iii)} \end{cases} \tag{7}$$

where for different cases μ and σ are given in (8).

Proof. The proof is based on (2)-(4) and [39, Theorems 1-3], where considering Cases 1-4 the random variable $Z(t) = \log|\mathbf{I}_{N_{\rm r}} + \frac{\phi}{N_{\rm t}}\mathbf{H}(t)\mathbf{H}(t)^h|$ converges in distribution to a Gaussian random variable $Y \sim \mathcal{N}(\mu, \sigma^2)$ which, depending on the numbers of antennas, has the following characteristics

$$(\mu,\sigma^2) = \begin{cases} \left(N_{\rm t}\log\left(1+\frac{N_{\rm r}\phi}{N_{\rm t}}\right), \frac{N_{\rm t}}{N_{\rm r}}\right), & \text{if Case 1} \\ \left(N_{\rm r}\log\left(1+\phi\right), \frac{N_{\rm r}\phi^2}{N_{\rm t}(1+\phi)^2}\right), & \text{if Case 2} \\ \left(N_{\rm r}\phi, \frac{N_{\rm r}}{N_{\rm t}}\phi^2\right), & \text{if Case 3} \\ \left(\tilde{\mu}, \tilde{\sigma}^2\right), & \text{if Case 4} \end{cases}$$

$$\tilde{\mu} = N_{\min}\log\left(\frac{\phi}{N_{\rm t}}\right) + N_{\min}\left(\sum_{i=1}^{N_{\max}-N_{\min}}\frac{1}{i} - \gamma\right) + \sum_{i=1}^{N_{\min}-1}\frac{i}{N_{\max}-i},\ \gamma = 0.5772\ldots$$

$$\tilde{\sigma}^2 = \sum_{i=1}^{N_{\min}-1}\frac{i}{(N_{\max}-N_{\min}+i)^2} + N_{\min}\left(\frac{\pi^2}{6} - \sum_{i=1}^{N_{\max}-1}\frac{1}{i^2}\right),$$

$$N_{\max} \doteq \max(N_{\rm t}, N_{\rm r}),\ N_{\min} \doteq \min(N_{\rm t}, N_{\rm r}). \tag{8}$$

In this way, from (2) and for different cases, the outage probability in fast-fading condition is given by

$$\Pr(\text{Outage})^{\text{Fast-fading}} = \Pr\left(Z \le \frac{R}{M}\right), Z \doteq \frac{1}{MT}\sum_{t=1}^{MT} Z(t), \tag{9}$$

where, because Z is the average of MT independent Gaussian random variables $Y \sim \mathcal{N}(\mu, \sigma^2)$, we have $Z \sim \mathcal{N}(\mu, \frac{1}{MT}\sigma^2)$. Consequently, using the cumulative distribution function (CDF) of Gaussian random variables, the outage probability in fast-fading condition is given by (7.i). The same arguments can be applied to derive (7.ii-iii) in slow-fading and quasi-static conditions. ■

The advantage of Lemma 1 is that, as seen in the following, it replaces the complicated optimization problem (5) by finding the solution of very simple equations with no need for derivatives or other optimization techniques. Then, as we show in Section V, in all cases the derived analytical results match with the ones found via simulations with very high accuracy. Moreover, Lemma 1 leads to the following corollaries:

1) For Cases 1-4, using INR MIMO-HARQ in the quasi-static, slow- and fast-fading channels leads to scaling the variance of the equivalent random variable by 1, M and MT, respectively. That is, using HARQ, there exists mappings between the quasi-static, the slow- and the fast-fading conditions in the sense that with proper scaling of σ in (7) they lead to the same outage probability.
2) With asymptotically large numbers of transmit and/or receive antennas, the optimal data rate which leads to zero outage probability and maximum throughput is given by $R = \mu - \omega, \omega \to 0$, with μ derived in (8); Interestingly, the result is independent of the fading condition. Also, with asymptotically high number of antennas and $R = \mu - \omega, \omega \to 0$, no HARQ is needed because the message is decoded in the first round (with probability 1).
3) Finally, using (7), we can map the MIMO-HARQ system into an equivalent SISO-HARQ setup whose fading follows $\mathcal{N}(\mu, \sigma^2)$ with μ and σ given in (8) for different cases.

[2] In [34], [35], which study multi-user MIMO setups, $N_{\rm t}$ and $N_{\rm r}$ are supposed to follow (6) while, as opposed to our work, they are considered to be asymptotically large.

Using Lemma 1, the minimum numbers of antennas satisfying different outage probability constraints are determined as stated in Theorem 1.

Theorem 1: The minimum numbers of the transmit and/or receive antennas in an INR MIMO-HARQ system that satisfy the outage probability constraint $\Pr(\text{Outage}) \leq \theta$ are given by

$$\begin{cases} \hat{N}_{\mathrm{r}} = \left\lceil \frac{\left(Q^{-1}(\theta)\right)^2}{4MTN_{\mathrm{t}}W^2\left(\frac{Q^{-1}(\theta)\sqrt{\phi}}{2\sqrt{MTN_{\mathrm{t}}}}e^{-\frac{R}{2MN_{\mathrm{t}}}}\right)} \right\rceil, & \text{if Case 1} \\ \hat{N}_{\mathrm{t}} = \left\lceil \left(\frac{\phi\sqrt{N_{\mathrm{r}}}Q^{-1}(\theta)}{\sqrt{MT}(1+\phi)\left(N_{\mathrm{r}}\log(1+\phi)-\frac{R}{M}\right)} \right)^2 \right\rceil, & \text{if Case 2} \\ \hat{N}_{\mathrm{r}} = \left\lceil \hat{N} \right\rceil, \hat{N}_{\mathrm{t}} = \left\lceil K\hat{N} \right\rceil, \hat{N} = \frac{R}{M\phi} + \frac{Q^{-1}(\theta)}{\sqrt{MTK}}, & \text{if Case 3} \\ \hat{N}_{\mathrm{r}} = \left\lceil \hat{N} \right\rceil, \hat{N}_{\mathrm{t}} = \left\lceil K\hat{N} \right\rceil & \text{if Case 4} \end{cases}$$

$$\begin{cases} \hat{N} \simeq \frac{\frac{R}{M}+\frac{Q^{-1}(\theta)}{\sqrt{MT}}\sqrt{\log\left(\frac{K}{K-1}\right)}}{\log(\phi)-\gamma-1+(K-1)\log\left(\frac{K}{K-1}\right)}, & K > 1 \\ \hat{N} \simeq \frac{\frac{R}{M}+\frac{Q^{-1}(\theta)}{\sqrt{MT}}\sqrt{-\log(1-K)}}{K\left(\log(\phi)-\gamma-1-\log(K)+\left(\frac{K-1}{K}\right)\log(1-K)\right)} & K < 1, \end{cases} \tag{10}$$

if the channel is fast-fading. For the slow-fading and quasi-static conditions, the minimum numbers of the antennas are obtained by (10) where the term $\frac{Q^{-1}(\theta)}{\sqrt{MT}}$ is replaced by $\frac{Q^{-1}(\theta)}{\sqrt{M}}$ and $Q^{-1}(\theta)$, respectively.

Proof. See Appendix A. ■

According to Theorem 1, the following conclusions can be drawn:

1) Using the second order Taylor approximation $W(e^{a-bx}) \simeq c_0 + c_1(a-bx) + c_2(a-bx)^2$, $c_0 = 0.5671, c_1 = 0.3619, c_2 = 0.0737, \forall a, b$, in (10), the required number of receive antennas in Case 1 is rephrased as

$$\begin{aligned} \hat{N}_{\mathrm{r}} &\simeq \left\lceil \frac{\left(Q^{-1}(\theta)\right)^2}{\Delta_0} \right\rceil \\ &\simeq \left\lceil \frac{\left(Q^{-1}(\theta)\right)^2}{4MTN_{\mathrm{t}}\left(c_0 + c_1\left(\log\left(\frac{Q^{-1}(\theta)\sqrt{\phi}}{2\sqrt{MTN_{\mathrm{t}}}}\right) - \frac{R}{2MN_{\mathrm{t}}}\right)\right)^2} \right\rceil, \\ \Delta_0 &= 4MTN_{\mathrm{t}}\Bigg(c_0 + c_1\left(\log\left(\frac{Q^{-1}(\theta)\sqrt{\phi}}{2\sqrt{MTN_{\mathrm{t}}}}\right) - \frac{R}{2MN_{\mathrm{t}}}\right) \\ &\quad + c_2\left(\log\left(\frac{Q^{-1}(\theta)\sqrt{\phi}}{2\sqrt{MTN_{\mathrm{t}}}}\right) - \frac{R}{2MN_{\mathrm{t}}}\right)^2\Bigg)^2, \end{aligned} \tag{11}$$

where the last approximation holds for moderate/high SNRs. Thus, ignoring the small terms in the denominator of (11), at moderate/high SNRs the required number of receive antennas increases with $(Q^{-1}(\theta))^2$ (almost) linearly. On the other hand, the required number of receive antennas is inversely proportional to the number of experienced fading realizations MT, the number of transmit antennas N_{t}, and $(\log(\phi))^2$. Interestingly, we can use (10.Case 2) to show that at high SNRs the same scaling laws hold for Cases 1 and 2. That is, in Case 2, the required number of transmit antennas decreases (resp. increases) with MT, N_{t}, and $(\log(\phi))^2$ (resp. $(Q^{-1}(\theta))^2$) linearly.

2) The same scaling laws are valid in Cases 3 and 4, i.e., when the numbers of transmit and receive antennas increase simultaneously. For instance, the required number of antennas increases with $Q^{-1}(\theta)$ and the code rate R affinely[3] (see (10.Cases 3-4)). At hard outage probability constraints, i.e., small values of θ, the required number of antennas decreases with the number of retransmissions according to $\frac{1}{\sqrt{M}}$. On the other hand, the number of antennas decreases with M linearly when the outage constraint is relaxed, i.e., θ increases. The only difference between Cases 3 and 4 is that in Case 3 (resp. Case 4) the number of antennas decreases with ϕ (resp. $\log(\phi)$) linearly.
3) It has been previously proved that at low SNRs the same performance is achieved by the MIMO systems using INR and repetition time diversity (RTD) HARQ [14, Section V.B]. Thus, although the paper concentrates on the INR HARQ, the same number of antennas are required in the MIMO-RTD setups, as long as the SNR is low.

As the number of antennas increases, the CDF of the accumulated mutual information, e.g., $\frac{1}{MT}\sum_{n=1}^{M}\sum_{t=(n-1)T+1}^{nT}\log|\mathbf{I}_{N_{\mathrm{r}}} + \frac{\phi}{N_{\mathrm{t}}}\mathbf{H}(t)\mathbf{H}(t)^h|$ in fast-fading conditions, tends towards the step function. Therefore, depending on the SNR and the initial rate, the outage probability rapidly converges to either zero or one as the number of transmit and/or receiver antennas increases. To further elaborate on this point and investigate the effect of the number of antennas, we define the normalized outage factor as

$$\Gamma = -\frac{\log(\Pr(\text{Outage}))}{N_{\mathrm{t}}N_{\mathrm{r}}}. \tag{12}$$

Intuitively, (12) gives the negative of the slope of the outage probability curve plotted versus the product of the numbers of transmit/receive antennas. That is, the normalized outage factor shows how fast the outage probability scales with the number of transmit/receive antennas when they increase. Also, (12) follows the same concept as in the diversity gain $D = -\lim_{\phi\to\infty}\frac{\log(\Pr(\text{Outage}))}{\phi}$ [9, Eq. 14] which is an efficient metric for the asymptotic analysis of the MIMO setups. Theorem 2 studies the normalized outage factor in more details.

Theorem 2: For Cases 1-4, different fading conditions and appropriate initial rates/SNR, the normalized outage factor is approximated by (35).

Proof. See Appendix B. ■

Interestingly, the theorem indicates that:

1) As the number of antennas increases, the normalized outage factor becomes constant in all cases, except Case 1 with a given and large number of transmit and receive antennas, respectively. Intuitively, this is because in all cases (except Case 1) the power per transmit antenna decreases by increasing the number of transmit antennas. Therefore, there is a tradeoff between increasing the diversity and reducing the power per antenna and, as a result, the normalized outage factor converges to the values given in (35). In Case 1, however, the message

[3]The variable y is affine with x if $y = a + bx$ for given constants a and b.

decoding probability is always increased by increasing the number of receive antennas and, as seen in Theorem 2, the normalized outage factor increases with $N_{\rm r}$ monotonically, as long as $\mu \geq \frac{R}{M}$.

2) In Case 3, the normalized outage factor becomes independent of the transmission SNR as long as $\mu \geq \frac{R}{M}$. In Cases 1, 2 and 4, on the other hand, the normalized outage factor scales with the SNR according to $(\log(\phi))^2$, if the SNR is high.
3) In all cases, the normalized outage factor scales with the number of experienced fading realizations during the packet transmission, i.e., MT, linearly. Note that the same conclusion has been previously derived for the diversity gain $D = -\lim_{\phi\to\infty} \frac{\log(\Pr(\text{Outage}))}{\phi}$ [10], [12].
4) In cases 3-4, the normalized outage factor does not depend on the initial transmission rate. Moreover, in Case 3 the normalized outage factor is independent of the ratio between the number of transmit and receive antennas.

A. On the Effect of Power Amplifiers

As the number of the transmit antennas increases, it is important to take the efficiency of radio-frequency PAs into account [36]–[38]. For this reason, we use Lemma 1 to investigate the system performance in the cases with non-ideal PAs as follows.

It has been previously shown that the PA efficiency can be written as [48], [49], [50, Eq. (3)]

$$\frac{\phi}{\phi^{\rm cons}} = \epsilon \left(\frac{\phi}{\phi^{\rm max}}\right)^{\vartheta} \Rightarrow \phi = \sqrt[1-\vartheta]{\frac{\epsilon \phi^{\rm cons}}{(\phi^{\rm max})^{\vartheta}}}. \quad (13)$$

Here, $\phi, \phi^{\rm max}$ and $\phi^{\rm cons}$ are the output, the maximum output, and the consumed power of the PA, respectively, $\epsilon \in [0,1]$ denotes the maximum power efficiency achieved at $\phi = \phi^{\rm max}$, and ϑ is a parameter that, depending on the PA classes, varies between $[0,1]$. Note that in (13) the parameter $\phi^{\rm max}$ has different effects, as it implies a maximum output power constraint $\phi \leq \phi^{\rm max}$ and also affects the PAs maximum consumed power by $\phi^{\rm cons,max} = \frac{\phi^{\rm max}}{\epsilon}$. In this way, and because the INR-based MIMO-HARQ setup can be mapped into an equivalent SISO-HARQ system (see Lemma 1 and its following discussions), the equivalent mean and variances (8) are rephrased as

$$(\mu, \sigma^2) = \begin{cases} \left(N_{\rm t} \log\left(1 + \frac{N_{\rm r}}{N_{\rm t}} \sqrt[1-\vartheta]{\frac{\epsilon\phi^{\rm cons}}{(\phi^{\rm max})^{\vartheta}}}\right), \frac{N_{\rm t}}{N_{\rm r}}\right), & \text{Case 1} \\ \left(N_{\rm r} \log\left(1 + \sqrt[1-\vartheta]{\frac{\epsilon\phi^{\rm cons}}{(\phi^{\rm max})^{\vartheta}}}\right), \frac{N_{\rm r}}{N_{\rm t}\left(1+\sqrt[1-\vartheta]{\frac{(\phi^{\rm max})^{\vartheta}}{\epsilon\phi^{\rm cons}}}\right)^2}\right), & \text{Case 2} \\ \left(N_{\rm r} \sqrt[1-\vartheta]{\frac{\epsilon\phi^{\rm cons}}{(\phi^{\rm max})^{\vartheta}}}, \frac{N_{\rm r}}{N_{\rm t}} \sqrt[1-\vartheta]{\left(\frac{\epsilon\phi^{\rm cons}}{(\phi^{\rm max})^{\vartheta}}\right)^2}\right), & \text{Case 3} \\ (\tilde{\mu}, \tilde{\sigma}^2), & \text{Case 4} \end{cases}$$

$$\tilde{\mu} = N_{\rm min} \log\left(\frac{1}{N_{\rm t}} \sqrt[1-\vartheta]{\frac{\epsilon\phi^{\rm cons}}{(\phi^{\rm max})^{\vartheta}}}\right) + N_{\rm min}\left(\sum_{i=1}^{N_{\rm max}-N_{\rm min}} \frac{1}{i} - \gamma\right) + \sum_{i=1}^{N_{\rm min}-1} \frac{i}{N_{\rm max}-i},$$

$$\tilde{\sigma}^2 = \sum_{i=1}^{N_{\rm min}-1} \frac{i}{(N_{\rm max}-N_{\rm min}+i)^2} + N_{\rm min}\left(\frac{\pi^2}{6} - \sum_{i=1}^{N_{\rm max}-1} \frac{1}{i^2}\right),$$
$$N_{\rm max} = \max(N_{\rm t}, N_{\rm r}),\ N_{\rm min} = \min(N_{\rm t}, N_{\rm r}),\ \gamma = 0.5772\ldots. \quad (14)$$

in the cases with non-ideal PAs. This is the only modification required for the non-ideal PA scenario and the rest of the analysis remains the same as before.

B. On the Effect of Power Allocation

Throughout the paper, we studied the system performance assuming a peak power constraint at the transmitter. However, the system performance is improved if the transmission powers are updated in the HARQ retransmission rounds.

Let the transmission power in the mth round be ϕ_m. Then, the outage probability in the fast-fading condition[4], i.e., (2), is rephrased as

$$\Pr(\text{Outage})^{\text{Fast-fading}} = \Pr\left(\frac{1}{MT}\sum_{m=1}^{M}\sum_{t=(m-1)T+1}^{mT} \log\left|\mathbf{I}_{N_{\rm r}} + \frac{\phi_m}{N_{\rm t}}\mathbf{H}(t)\mathbf{H}(t)^h\right| \leq \frac{R}{M}\right)$$
$$\overset{(a)}{=} \Pr\left(\frac{1}{MT}\sum_{m=1}^{M} Z_m \leq \frac{R}{M}\right) \overset{(b)}{=} Q\left(\frac{\bar{\mu}_{(M)} - \frac{R}{M}}{\bar{\sigma}_{(M)}}\right),$$
$$\bar{\mu}_{(m)} = \frac{1}{m}\sum_{n=1}^{m}\mu_n, \bar{\sigma}^2_{(m)} = \frac{1}{Tm^2}\sum_{n=1}^{m}\sigma_n^2, \quad (15)$$

where μ_n and σ_n are obtained by replacing ϕ_n into (8). Here, (a) is obtained by $Z_m \doteq \sum_{t=(m-1)T+1}^{mT} \log|\mathbf{I}_{N_{\rm r}} + \frac{\phi_m}{N_{\rm t}}\mathbf{H}(t)\mathbf{H}(t)^h| \sim \mathcal{N}(T\mu_m, T\sigma_m^2)$. Also, (b) is based on the fact that the sum of independent Gaussian random variables is a Gaussian random variable with the mean and variance equal to the sum of the variables means and variances, respectively.

If the message is correctly decoded in the mth round, the total transmission energy and the total number of channel uses are $\xi_{(m)} = L\sum_{n=1}^{m}\phi_n$ and $l_{(m)} = mL$, respectively. Also, the total transmission energy and the number of channel uses are $\xi_M = L\sum_{n=1}^{M}\phi_M$ and $l_{(M)} = ML$ if an outage occurs, where all possible retransmission rounds are used. Thus, we can follow the same procedure as in [5], [6], [14] to find the average power, defined as the expected transmission energy over the expected number of channel uses, as

$$\bar{\Phi} = \frac{d_0}{d_1} = \frac{\phi_1 + \sum_{m=1}^{M-1}\phi_{m+1} Q\left(\frac{\bar{\mu}_{(m)} - \frac{R}{m}}{\bar{\sigma}_{(m)}}\right)}{1 + \sum_{m=1}^{M-1} Q\left(\frac{\bar{\mu}_{(m)} - \frac{R}{m}}{\bar{\sigma}_{(m)}}\right)},$$
$$d_0 \doteq \phi_1 + \sum_{m=1}^{M-1}\left(\phi_{m+1}\times \Pr\left(\frac{1}{Tm}\sum_{n=1}^{m}\sum_{t=(n-1)T+1}^{nT} \log\left|\mathbf{I}_{N_{\rm r}} + \frac{\phi_n}{N_{\rm t}}\mathbf{H}(t)\mathbf{H}(t)^h\right| \leq \frac{R}{m}\right)\right),$$

[4]For simplicity, the results of this part are given mainly for the fast-fading condition. It is straightforward to extend the results to the cases with other fading models.

$$d_1 \doteq 1+ \sum_{m=1}^{M-1} \Pr\left(\frac{1}{Tm}\sum_{n=1}^{m}\sum_{t=(n-1)T+1}^{nT} \log\left|\mathbf{I}_{N_\mathrm{r}} + \frac{\phi_n}{N_\mathrm{t}}\mathbf{H}(t)\mathbf{H}(t)^h\right| \le \frac{R}{m}\right). \tag{16}$$

In this way, with a power constraint $\bar{\Phi} \le \phi$, the problem formulation (5) is rephrased as

$$\begin{aligned} \{\hat{N}_\mathrm{t}, \hat{N}_\mathrm{r}\} &= \arg\min_{N_\mathrm{t},N_\mathrm{r}} \{\Pr(\text{Outage}) \le \theta\} && \text{(i)} \\ &\text{s.t.} \bar{\Phi} \le \phi, && \text{(ii)} \end{aligned} \tag{17}$$

which, using (8) and (15), can be solved numerically. Following the same discussions as in, e.g., [7], [8], [13], it can be shown that the problem of optimal power allocation between the HARQ transmissions is a complex non-convex problem and does not have a closed-form expression even in the simplest case of SISO setups. However, Theorem 3 shows the optimality of uniform power allocation at low/moderate SNRs. The result of the theorem is interesting because it holds for different cases and the range of SNR which is of interest as the number of antennas increases.

Theorem 3: At low SNRs and for Cases 1-3, the optimal power allocation, in terms of (17), tends towards uniform power allocation, i.e., $\phi_i = \phi_j, \forall i, j$.

Proof. See Appendix C. ■

The accuracy of the results in Theorem 3 is verified in Section V (Fig. 6b). Finally, note that, as an efficient numerical optimization algorithm, one can use the machine learning-based algorithm of [5, Algorithm 1] with straightforward modifications to find the (sub)optimal retransmission powers, in terms of (17).

C. Finite Block-length Analysis with Erroneous Feedback and no CSI at the Receiver

Throughout the paper, we presented the results for the cases with long sub-codewords, perfect CSI at the receiver and error-free feedback in harmony with the literature. In this section, we relax these assumptions, and analyze the system performance in the cases with short packets, no CSI at the receiver and erroneous feedback. Particularly, following the same discussions as in [51], the outage probability of HARQ protocols with imperfect feedback channel is given by

$$\begin{aligned} &\Pr\left(\text{Outage}\right)^{\text{erroneous feedback}} \\ &= p_\mathrm{e} \sum_{m=1}^{M-1} \left(1-p_\mathrm{e}\right)^{m-1} \Pr\left(\mathcal{O}_m\right) + \left(1-p_\mathrm{e}\right)^{M-1} \Pr\left(\mathcal{O}_M\right). \end{aligned} \tag{18}$$

Here, p_e represents the feedback error probability and $\mathcal{O}_m$ is the event that the message is not correctly decoded up to the end of round m. Thus, to analyze the system performance, we need to find $\Pr\left(\mathcal{O}_m\right), \forall m$.

In [40], Polyanskiy, *et al.* presented tight bounds for the maximum achievable rates of finite-length codewords. Then, with no CSI at the receiver, [41] extended the results of [40] to quasi-static conditions and presented a very tight approximation for the the error probability of a code with codewords of finite length L and q information nats per codeword as [41, eq. (59)]

$$\begin{aligned} \delta(L,q) &= E\left[Q\left(\frac{\sqrt{L}\left(C(\mathbf{H}) - \frac{q}{L}\right)}{\sqrt{V(\mathbf{H})}}\right)\right], \\ C(\mathbf{H}) &= \log\left|\mathbf{I}_{N_\mathrm{r}} + \frac{\phi}{N_\mathrm{t}}\mathbf{H}\mathbf{H}^h\right|, \\ V(\mathbf{H}) &= \min(N_\mathrm{t}, N_\mathrm{r}) - \sum_{j=1}^{\min(N_\mathrm{t},N_\mathrm{r})} \frac{1}{(1+\frac{\phi}{N_\mathrm{t}}\lambda_j)^2}. \end{aligned} \tag{19}$$

Here, $\{\lambda_j\}$'s denote the eigenvalues of $\mathbf{H}\mathbf{H}^h$. From (19), the probability $\Pr(\mathcal{O}_m)$ is found as

$$\Pr(\mathcal{O}_m) = E\left[Q\left(\frac{\sqrt{mL}\left(C(\mathbf{H}) - \frac{q}{mL}\right)}{\sqrt{V(\mathbf{H})}}\right)\right], \tag{20}$$

which is based on the fact that 1) with a quasi-static condition, the same fading realization is experienced in all rounds of a packet, 2) the receiver combines all received signals of a packet to decode the message and, 3) for a given value of $\mathbf{H}$ and q nats, $\frac{\sqrt{L}\left(C(\mathbf{H})-\frac{q}{L}\right)}{\sqrt{V(\mathbf{H})}}$ is an increasing function of L and, thus, $\mathcal{O}_m \subset \mathcal{O}_n, n < m$ for quasi-static channels. Then, using $V(\mathbf{H}) \simeq \min(N_\mathrm{t}, N_\mathrm{r})$ and the linear approximation

$$Q(a_m(x-b_m)) \simeq \begin{cases} 1 & x \le b_m + \frac{1}{2a_m}, \\ \frac{1}{2} + a_m(x-b_m) & x \in \left[b_m + \frac{1}{2a_m}, b_m - \frac{1}{2a_m}\right], \\ 0 & x \ge b_m - \frac{1}{2a_m}, \end{cases} \forall a_m, b_m, m, \tag{21}$$

with $a_m = -\sqrt{\frac{mL}{2\pi\min(N_\mathrm{t},N_\mathrm{r})}}$ and $b_m = \frac{q}{mL}$, we have

$$\begin{aligned} &\Pr(\mathcal{O}_m) \simeq E\left[Q\left(\frac{\sqrt{mL}\left(\log\left|\mathbf{I}_{N_\mathrm{r}} + \frac{\phi}{N_\mathrm{t}}\mathbf{H}\mathbf{H}^h\right| - \frac{q}{mL}\right)}{\sqrt{\min(N_\mathrm{t},N_\mathrm{r})}}\right)\right] \\ &\overset{(c)}{\simeq} \int_0^\infty f_Z(x) Q\left(a_m\left(x-b_m\right)\right) \mathrm{d}x \\ &= \int_0^{b_m+\frac{1}{2a_m}} f_Z(x)\mathrm{d}x + \left(\frac{1}{2} - a_m b_m\right) \int_{b_m+\frac{1}{2a_m}}^{b_m-\frac{1}{2a_m}} f_Z(x)\mathrm{d}x \\ &+ a_m \int_{b_m+\frac{1}{2a_m}}^{b_m-\frac{1}{2a_m}} x f_Z(x)\mathrm{d}x \\ &\overset{(d)}{\simeq} Q\left(\frac{\mu - b_m - \frac{1}{2a_m}}{\sigma}\right) \\ &+ \left(\frac{1}{2} - a_m b_m\right)\left(Q\left(\frac{\mu - b_m + \frac{1}{2a_m}}{\sigma}\right) - Q\left(\frac{\mu - b_m - \frac{1}{2a_m}}{\sigma}\right)\right) \\ &+ \left(a_m b_m - \frac{1}{2}\right) Q\left(\frac{\mu - b_m + \frac{1}{2a_m}}{\sigma}\right) \\ &- \left(\frac{1}{2} + a_m b_m\right) Q\left(\frac{\mu - b_m - \frac{1}{2a_m}}{\sigma}\right) + Q\left(\frac{\mu - b_m}{\sigma}\right). \end{aligned} \tag{22}$$

Here, $f_Z(\cdot)$ and $F_Z(\cdot)$ represent the PDF and the CDF of the auxiliary random variable Z defined in Lemma 1. Also, (c) comes from the linear approximation technique of (21) and partial integration. Finally, (d) follows from the

first order Riemann integral approximation $\int_{a_0}^{a_1} f(x)\mathrm{d}x \simeq (a_1-a_0)f\left(\frac{a_0+a_1}{2}\right)$ and the CDF $F_Z(x) = Q\left(\frac{\mu-x}{\sigma}\right)$ with (μ,σ) given by Theorem 1 for different Cases 1-4.

In this way, replacing (22) into (18) and using the means and variances given by Theorem 1 for Cases 1-4, we can represent the outage probability of the MIMO-HARQ setup with no CSI at the receiver, erroneous feedback and finite length codewords as a function of the number of transmit and receive antennas. Thus, in all Cases 1-4 the minimum number of transmit and/or receiver antennas can be easily derived by, e.g., "fsolve" function of MATLAB because the outage probability (18) is represented as a function of a single unknown variable, e.g., N_r in Case 1. In Figs. 7-8 we study the system performance for different codeword lengths/feedback error probabilities, and validate the accuracy of the approximations proposed in (21)-(22) by comparing them with the corresponding exact values that can be evaluated numerically.

To close the discussions it is worth noting that, as opposed to throughput-based applications, the HARQ feedback delay does not affect the performance of outage-constrained systems, e.g., [7], [8], [13]. For this reason, we have not considered the effect of delayed feedback in our analysis. Finally, taking the feedback delay into account, we have previously shown that even with the throughput as the objective function the performance of HARQ protocols is not sensitive to the feedback delay for a large range of parameter settings/SNRs [52].

V. Simulation Results and Discussions

In this section, we verify the accuracy of the derived results, and present the simulation results in independent and spatially/temporally correlated fading conditions as follows.

A. Performance Analysis in Spatially/Temporally independent Fading Conditions

In Figs. 1-4, we derive the required number of transmit/receive antennas in outage-limited conditions, and verify the accuracy of the results in Theorem 1 and (11). Particularly, the figures compare the required number of antennas derived via Theorem 1 and exhaustive search (in all figures, we have considered 2×10^7 different channel realizations for each point in the simulation curves). Also, for faster convergence, we have repeated the simulations by using the iterative algorithm of [5, Algorithm 1]. In all cases, the results of the exhaustive search-based scheme and the iterative algorithm of [5, Algorithm 1] are the same with high accuracy, which is an indication of reliable results. Setting $M=2, N_\mathrm{t}=1$ (Case 1), and the outage probability constraints $\Pr(\text{Outage}) \leq \theta$ (with $\theta = 10^{-4}, 10^{-2}$), Fig. 1 shows the required number of receive antennas versus the initial transmission rate R. The results of the figure are obtained for slow-fading conditions and different transmission SNRs. Then, considering $N_\mathrm{r}=1$ or 2, Fig. 2 demonstrates the required number of transmit antennas in Case 2 with large N_t and given N_r. Here, we consider quasi-static, slow- and fast-fading conditions with $\theta=10^{-4}, T=2, M=2, \phi=15$ dB. In Fig. 3, we verify the effect of HARQ on the system performance. Here, assuming Case 1 (large N_r and $N_\mathrm{t}=1,5$), the required number of antennas is derived in the scenarios with ($M=2$) and without ($M=1$) HARQ. The results of the figure are given for quasi-static channels, $\phi=5$ dB and $\theta=10^{-4}$.

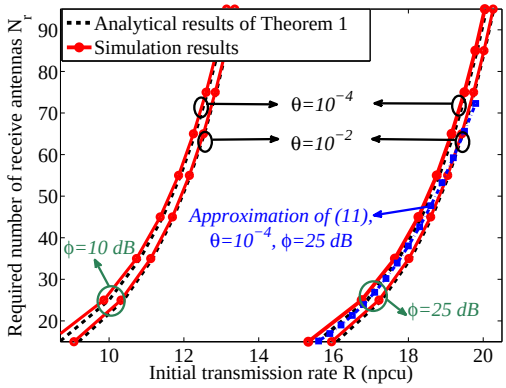

Figure 1. The required number of receive antennas vs the initial transmission rate R (Case 1: large N_r, given N_t). Outage probability constraint $\Pr(\text{Outage}) < \theta$ ($\theta = 10^{-4}$ or 10^{-2}), slow-fading conditions, $M=2$, and $N_\mathrm{t}=1$.

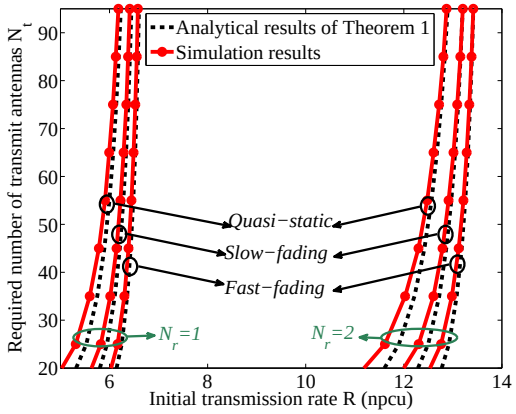

Figure 2. The required number of transmit antennas vs the initial transmission rate R for the quasi-static, slow- and fast-fading conditions (Case 2: large N_t, given N_r). Outage probability constraint $\Pr(\text{Outage}) < \theta$, ($\theta = 10^{-4}$), $\phi = 15$ dB, $T=2, M=2$, and $N_\mathrm{r}=1$ or 2.

Figure 4 studies the required number of antennas in Cases 3 and 4 with low and high SNRs, respectively, large number of transmit and receive antennas, and $\frac{N_\mathrm{t}}{N_\mathrm{r}} = K$. Also, the figure demonstrates the analytical results of Theorem 1 when the approximation steps $(c)-(d)$ of (28)-(29) are not implemented, i.e., (24) is solved numerically via (8). Here, we consider quasi-static conditions, $M=1$, and $\theta=10^{-3}$. Note that, to have the simulation results of Case 4 in reasonable running time, we have stopped the simulations at moderate initial transmission rates. For this reason, the simulation results of Case 4, i.e., the solid-line curves of Case 4 in Fig. 4, are plotted for the moderate initial rates.

In Fig. 5, we analyze the normalized outage factor and evaluate the theoretical results of Theorem 2. Considering quasi-static conditions, $M=1, N_\mathrm{t}=1$ and $\phi=5$ dB, Fig. 5a shows the outage probability versus the product of the number of transmit and receive antennas. Also, Fig. 5b demonstrates the normalized outage factor in Case 1 and compares the results with the theoretical derivations of Theorem 2. Finally, Fig. 5c studies the outage probability in Case 2 and compares the

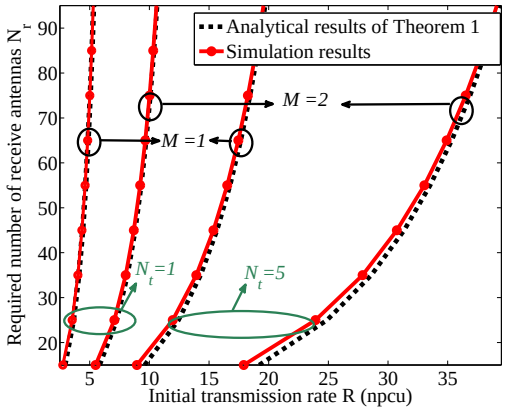

Figure 3. The required number of transmit antennas in the scenarios with HARQ ($M = 2$) and without HARQ ($M = 1$), Case 1: (large $N_{\rm r}$, given $N_{\rm t}$). Outage probability constraint $\Pr(\text{Outage}) < \theta$ with $\theta = 10^{-4}$, $\phi = 5$ dB, , $N_{\rm t} = 1$ or 5, and quasi-static conditions.

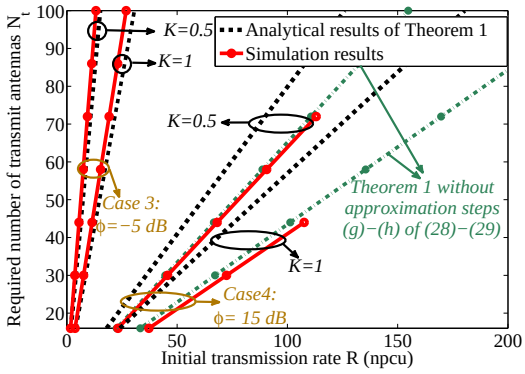

Figure 4. The required number of transmit antennas vs the initial transmission rate, Cases 3 and 4: (large $N_{\rm t}, N_{\rm r}$, $\frac{N_{\rm t}}{N_{\rm r}} = K$). Outage probability constraint $\Pr(\text{Outage}) < \theta$ with $\theta = 10^{-3}$, $\phi = -5$ or 15 dB, , $M = 1$, and quasi-static conditions.

slope of the curves with the normalized outage factor derived in Theorem 2. Here, the results are obtained for the slow- and fast-fading conditions ($T = 2$) with $R = 1, M = 1, N_{\rm r} = 1$ and $\phi = 5$ dB.

Figure 6 evaluates the effect of non-ideal PAs and adaptive power allocation on the performance of large MIMO setups. Considering fast-fading conditions with $T = 2$, Case 2 with large (resp. given) number of transmit (resp. receive) antennas and the outage probability constraint $\Pr(\text{Outage}) \leq \theta, \theta = 10^{-4}$, Fig. 6a demonstrates the supported initial transmission rates, i.e., the maximum rates for which the outage probability is guaranteed, versus the total consumed power. For the non-ideal PA, we set $\phi^{\max} = 30$ dB, $\vartheta = 0.5, \epsilon = 0.65$, while the ideal PA corresponds to $\phi^{\max} \to \infty, \vartheta = 0, \epsilon = 1$ in (13). The figure demonstrates the simulation results while, with the parameter settings of the figure, the same (with high accuracy) results are obtained if the supported initial rates are derived analytically according to (14) (Also, see Fig. 2 for the tightness of approximations in Case 2). Moreover, assuming slow-fading conditions and Case 2 with $N_{\rm r} = 1, \theta = 10^{-3}, M = 2$, Fig. 6b verifies the accuracy of the results in Theorem 3 and compares the required number of transmit antennas in the scenarios with optimal and uniform power allocation between the HARQ retransmissions.

Considering Case 1 with $N_{\rm t} = 2$ and feedback error probability $p_{\rm e} = 10^{-1}$, Fig. 7 derives the required number of receive antennas for different codeword lengths, and verifies the accuracy of the approximations (21)-(22). Here, the results are obtained for $\Pr(\text{Outage}) < \theta, \theta = 10^{-3}$, $M = 2$, and $\phi = -5$ dB. Then, setting $N_{\rm r} = 2$, $K = 500, L = 1000$ and $\phi = -5$ dB, Fig. 8 demonstrates the required number of transmit antennas in Case 2 versus the feedback error probability probability $p_{\rm e}$. According to the results, the following conclusions can be drawn:

- For Cases 1-3 and different fading conditions, the analytical results of Theorem 1 and (11) are very tight for a broad range of initial transmission rates, outage probability constraints and SNRs (Figs. 1-3). Also, in Case 1 (resp. Case 2) the tightness of the approximations increases with the number of receive (resp. transmit) antennas (Figs. 1-2). Moreover, the approximation scheme of Theorem 1 can accurately determine the required number of antennas in Case 3 with different values of K. For Case 4, we can find the required number of antennas accurately through Theorem 1 when (24) is solved numerically via (8). As such, the approximations $(c) - (d)$ of (28)-(29) decrease the accuracy, although the curves still follow the same trend as in the simulation results. For instance, with different approximation approaches of Case 4, the required number of antennas increases with the initial rate linearly, in harmony with the simulation results (Fig. 4). The tightness of the approximations in Cases 3 (resp. Case 4) increases when the SNR decreases (resp. increases). Finally, the scaling laws of Theorem 1 are valid because, as demonstrated in Figs. 1-4, in all cases the analytical and the simulation results follow the same trends (see Theorem 1 and its following discussions).
- In all cases, better approximation is achieved via Theorem 1 in fast-fading (resp. slow-fading) conditions compared to slow-fading (resp. quasi-static) conditions. This is intuitively because the central limit Theorem provides better approximation in Lemma 1 when the number of experienced fading realizations increases.
- The required number of antennas decreases as the outage probability constraint is relaxed, i.e., θ increases, while for different transmission SNRs, there is (almost) a fixed gap between the curves of different outage probability constraints (Fig. 1). Also, fewer antennas are required when the number of fading realizations experienced during the HARQ packet transmission increases. Intuitively, this is because more diversity is exploited by the HARQ in the fast-fading (resp. slow-fading) condition compared to the slow-fading (resp. quasi-static) conditions and, consequently, different outage probability constraints are satisfied with fewer antennas in the fast-fading (resp. slow-fading) conditions (Fig. 2). However, the gap between the system performance in different fading conditions decreases with the number of antennas (Fig. 2).
- The HARQ reduces the required number of anten-

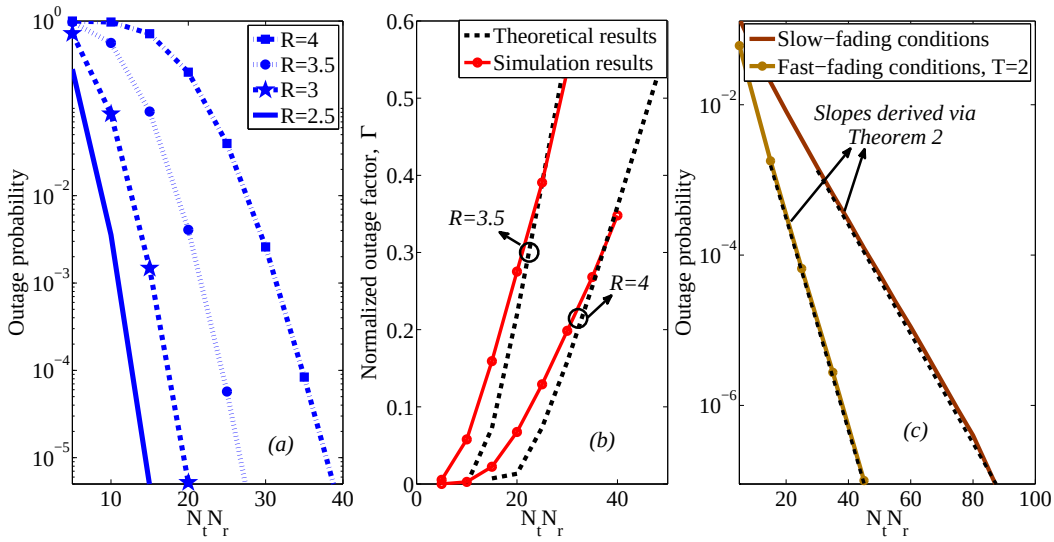

Figure 5. Subplot (a): The outage probability vs the product of the number of transmit and receive antennas, Case 1, $N_{\rm t}=1$, quasi-static conditions, $M=1, \phi=5$ dB. Subplot (b): The normalized outage factor vs the product of the number of transmit and receive antennas, Case 1, $N_{\rm t}=1$, quasi-static conditions, $M=1$, and $\phi=5$ dB. Subplot (c): The outage probability vs the product of the number of transmit and receive antennas, Case 2, $N_{\rm r}=1$, $M=1$, $\phi=5$ dB, and $R=1$.

nas significantly (Fig. 3). For instance, consider the quasi-static conditions, the outage probability constraint $\Pr(\text{Outage}) \leq 10^{-4}$, $N_{\rm t}=5$, $\phi=5$ dB and the code rate 20 npcu. Then, the implementation of HARQ with a maximum of $M=2$ retransmissions reduces the required number of receive antennas from 95 without HARQ to 15 (Fig. 3). Moreover, the effect of HARQ increases with the number of transmit/receive antennas (Fig. 3).

- Different outage probability requirements are satisfied with relatively few antennas. For instance, consider a SIMO setup in quasi-static conditions and $M=1, \phi=5$ dB. Then, with an initial rate $R=3$ npcu, the outage probabilities $\Pr(\text{Outage}) \leq 10^{-3}, 10^{-4}$ and 10^{-5} are satisfied with $16, 18$ and 20 receive antennas, respectively (Fig. 5a). These numbers increase to $31, 35$, and 38 for $R=4$ npcu (Fig. 5a).
- The normalized outage factor, i.e., the negative of the slope of the outage probability curve versus the product of the number of antennas as the number of antennas increases, follows the theoretical results of Theorem 2 with high accuracy (Figs. 5b and 5c). Also, the number of fading realizations experienced during the packet transmission increases the normalized outage factor linearly (Fig. 5c. Also, see Theorem 2 and its following discussions).
- The inefficiency of the PAs affects the performance of large MIMO setups remarkably. For instance, with the parameter settings of Fig. 6a and $R=10$ npcu, $N_{\rm r}=2$, the inefficiency of the PAs increases the consumed power by ~ 11 dB (Fig. 6a). However, the effect of the PAs inefficiency decreases with the SNR which is intuitively because the *effective* efficiency of the PAs $\epsilon^{\text{effective}} = \epsilon(\frac{\phi}{\phi^{\max}})^{\vartheta}$ is improved at high SNRs. On the other hand, in harmony with Theorem 3, optimal power allocation between the HARQ retransmissions reduces the required number of antennas marginally (Fig. 6b). Therefore, considering Theorem3/Fig. 6b and the implementation complexity of adaptive power allocation, uniform power allocation is a good choice for large MIMO systems at low SNRs.
- As demonstrated in Fig. 7, the finite block-length approximation results of (21)-(22) are very tight for moderate/large number of antennas. Moreover, for a given number of nats per codeword, increasing the number of antennas can effectively reduce the required codeword length leading to low data transmission delay. Finally, with few antennas, the system performance is remarkably affected by the feedback error probability (Fig. 8). However, the effect of erroneous feedback decreases when the number of antennas increases. This is intuitively because with large number of antennas the message is correctly decoded in the first retransmissions with high probability, and the sensitivity to feedback error decreases.

B. On the Effect of Spatial Correlation

Throughout the paper, we considered IID fading conditions motivated by the fact that the millimeter-wave communication, which will definitely be a part in the next generation of wireless networks, makes it possible to assemble many antennas close together with small spatial correlations [3], [4]. However, it is still interesting to analyze the effect of the antennas spatial correlation on the system performance. For this reason, we consider the spatially-correlated conditions with Kronecker spatial correlation model [53], [54] where, denoting the transmit- and the receive-side correlation matrices by $\Omega_{\rm t}$ and $\Omega_{\rm r}$, respectively, the channel matrix follows $\mathbf{H} \sim \mathcal{CN}(\mathbf{0}, \Omega_{\rm t} \bigotimes \Omega_{\rm r})$. Particularly, Fig. 9 demonstrates the required number of antennas in Case 2 with $N_{\rm r}=1$, $\Omega_{\rm r}=N_{\rm t}$ and $\Omega_t[i,j]=\beta^{|i-j|}, i,j=1,\ldots,N_{\rm t}$. Here, β is a correlation coefficient where $\beta=0$ (resp. $\beta=1$) corresponds to the uncorrelated (resp. fully correlated) conditions.

As shown in the figure, the effect of the antennas spatial correlation on the required number of antennas is negligible

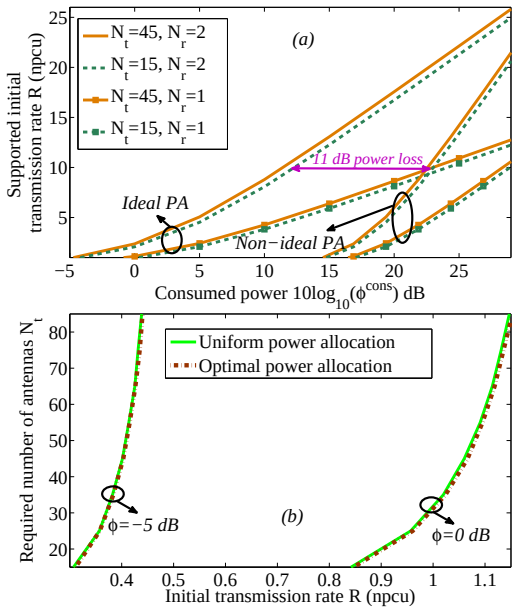

Figure 6. Subplot (a): On the effect of non-ideal PAs. Supported initial transmission rate vs the consumed power $10\log_{10}(\phi^{\text{cons}})$. Case 2: (large N_{t}, given N_{r}), outage probability constraint $\Pr(\text{Outage}) < \theta$, $\theta = 10^{-4}$, $T = 2, M = 2$, fast-fading conditions. In the cases with non-ideal PAs, we set $\epsilon = 0.65, \vartheta = 0.5, \phi^{\max} = 30$ dB. Subplot (b): On the effect of adaptive power allocation. The required number of transmit antennas vs the initial transmission rate R (npcu). Case 2: (large N_{t}, given N_{r}), outage probability constraint $\Pr(\text{Outage}) < \theta$ with $\theta = 10^{-3}$, $N_{\text{r}} = 1, \phi = -5$ or 0 dB, $M = 2$, and slow-fading conditions.

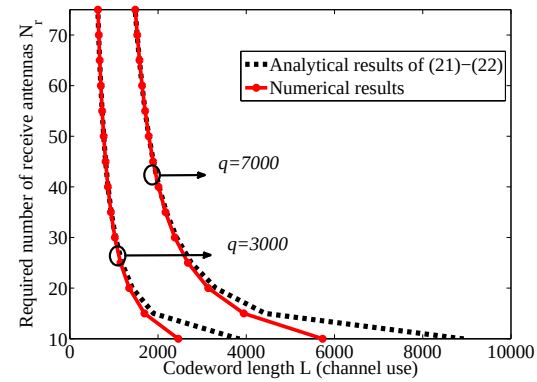

Figure 7. The required number of receive antennas vs the codeword length L (Case 1: large N_{r}, given N_{t}). Outage probability constraint $\Pr(\text{Outage}) < \theta$, $\theta = 10^{-3}$, $p_{\text{e}} = 10^{-1}$, $N_{\text{t}} = 2, M = 2$ quasi-static conditions and $\phi = -5$ dB.

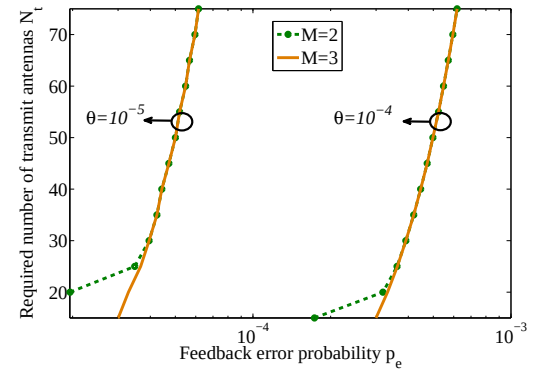

Figure 8. The required number of receive antennas vs the feedback error probability p_{e} (Case 2: large N_{t}, given N_{r}). Outage probability constraint $\Pr(\text{Outage}) < \theta\,(\theta = 10^{-5}$ or $10^{-4})$, quasi-static conditions, $M = 2, 3$, and $N_{\text{r}} = 2, K = 500, L = 1000, \phi = -5$ dB.

for correlation coefficients of, say, $\beta \lesssim 0.4$. This is in harmony with, e.g., [53], [54] which, with different problem formulations/metrics, derive the same conclusion about the effect of the antennas correlation on the system performance. Then, the sensitivity to the spatial correlation increases for large values of the correlation coefficients, and the required number of antennas increases with β. However, the important point is that the curves follow the same trend, for a large range of correlation coefficients (Fig. 9). Thus, with high accuracy, the same scaling laws as in the IID scenario also hold for the correlated conditions, as long as the correlation coefficient is not impractically high. Moreover, we observe the same conclusions in the other cases, although not demonstrated in the figure. Finally, it is worth noting that, as shown in [55], for moderate/large number of transmit and/or receive antennas and with appropriate mean and variance selection, the accumulated mutual information of the correlated MIMO setups follows Gaussian distributions with high accuracy. Therefore, one can use [55] and the same procedure as in our paper to derive closed-form expressions for the required number of antennas in the spatially-correlated MIMO-HARQ systems.

C. On the Effect of Temporal Correlation

In Section IV, we analyzed the system performance for quasi-static, slow- and fast-fading conditions with no temporal correlation between the successive fading realizations. To evaluate the effect of temporal correlations, Fig. 10 derives the supported initial code rate for a correlated slow-fading model in which the successive fading realizations follow

$$\mathbf{H}(t) = \nu\mathbf{H}(t-1) + \sqrt{1-\nu^2}\varpi, \varpi \sim \mathcal{CN}^{N_{\text{r}}\times N_{\text{t}}}. \qquad (23)$$

Here, ν is the temporal correlation factor where $\nu = 0$ (resp. $\nu = 1$) corresponds to the uncorrelated slow-fading (resp. quasi-static) conditions. This is a well-established model considered in the literature for different applications, e.g., [56].

As demonstrated in the figure, more time diversity is exploited by HARQ at low correlation coefficients and, consequently, the supported initial rate increases as ν decreases. However, for a broad range of temporal correlation coefficients, the system performance is (almost) insensitive to the temporal correlation. Moreover, the effect of temporal correlation decreases as the number of antennas increases (Fig. 10).

VI. Conclusion

This paper studied the required number of antennas satisfying different outage probability constraints in large but finite MIMO setups. We showed that different quality-of-service requirements can be satisfied with relatively few transmit/receiver antennas. Also, we derived closed-form expressions for the normalized outage factor which is defined as the negative of the slope of the outage probability curve plotted versus the product of number of antennas. As demonstrated, the required number of antennas decreases by the implementation of HARQ remarkably. The effect of temporal/spatial correlation on the required number of antennas is negligible for small/moderate correlation coefficients, while its effect increases in highly correlated conditions. Finally, with the

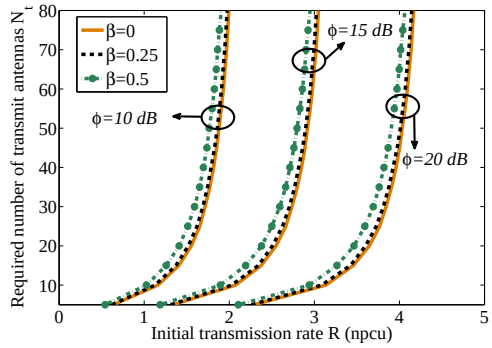

Figure 9. The required number of antennas in different spatially-correlated conditions. Case 2: (large $N_{\rm t}$, given $N_{\rm r}$), outage probability constraint $\Pr(\text{Outage}) < \theta$ with $\theta = 10^{-4}$, $M = 1$, quasi-static conditions, and $N_{\rm r} = 1$.

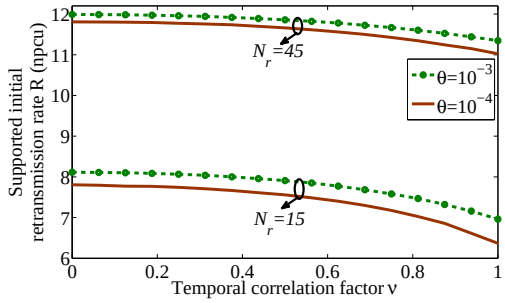

Figure 10. Supported initial rate vs the temporal correlation coefficient ν. (Case 1: large $N_{\rm r}$, given $N_{\rm t}$). Outage probability constraint $\Pr(\text{Outage}) < \theta$, ($\theta = 10^{-3}$ or 10^{-4}), $N_{\rm t} = 1, M = 3$ and $\phi = 2$ dB.

problem formulation of the paper, the performance of the large MIMO systems is sensitive (resp. almost insensitive) to the power amplifiers inefficiency (resp. adaptive power allocation between the HARQ retransmissions). Performance analysis in the cases with short packets and partial CSI at the receiver is an interesting extension of the work presented in this paper.

Appendix A
Proof of Theorem 1

Considering Lemma 1 and a fast-fading condition, (5) is rephrased as

$$\{\hat{N}_{\rm t}, \hat{N}_{\rm r}\}^{\text{Fast-fading}} = \arg\min_{N_{\rm t},N_{\rm r}} \left\{\Pr(\text{Outage})^{\text{Fast-fading}} \le \theta\right\} \overset{(e)}{=} \arg_{N_{\rm t},N_{\rm r}} \left\{\frac{\mu - \frac{R}{M}}{\sigma} = \frac{Q^{-1}(\theta)}{\sqrt{MT}}\right\}. \quad (24)$$

Here, (e) is obtained by Lemma 1 which, using the approximation results of (8), simplifies the optimization problem (5) to finding the solution for the equation given in (a). In this way, for different cases we have

Case 1[5]:

$$\hat{N}_{\rm r} = \arg_{N_{\rm r}} \left\{N_{\rm t}\log\left(1+\frac{N_{\rm r}\phi}{N_{\rm t}}\right) - \frac{R}{M} = \frac{Q^{-1}(\theta)}{\sqrt{MT}}\sqrt{\frac{N_{\rm t}}{N_{\rm r}}}\right\}$$
$$\overset{(f)}{\simeq} \frac{N_{\rm t}}{\phi}\arg_{u}\left\{\log(u) = \frac{R}{MN_{\rm t}} + \frac{Q^{-1}(\theta)\sqrt{\phi}}{\sqrt{MT}N_{\rm t}\sqrt{u}}\right\}$$
$$\Rightarrow \hat{N}_{\rm r} = \left\lceil \frac{(Q^{-1}(\theta))^2}{4MTN_{\rm t}W^2\left(\frac{Q^{-1}(\theta)\sqrt{\phi}}{2\sqrt{MT}N_{\rm t}}e^{-\frac{R}{2MN_{\rm t}}}\right)}\right\rceil \quad (25)$$

[5]For further approximation of the number of antennas in Case 1 see (11).

Case 2:

$$\hat{N}_{\rm t} = \arg_{N_{\rm t}}\left\{N_{\rm r}\log(1+\phi) - \frac{R}{M} = \frac{Q^{-1}(\theta)\phi\sqrt{N_{\rm r}}}{\sqrt{MT}(1+\phi)\sqrt{N_{\rm t}}}\right\}$$
$$\Rightarrow \hat{N}_{\rm t} = \left\lceil\left(\frac{\phi\sqrt{N_{\rm r}}Q^{-1}(\theta)}{\sqrt{MT}(1+\phi)\left(N_{\rm r}\log(1+\phi) - \frac{R}{M}\right)}\right)^2\right\rceil. \quad (26)$$

Case 3: $\hat{N}_{\rm r} = \left\lceil\hat{N}\right\rceil, \hat{N}_{\rm t} = \left\lceil K\hat{N}\right\rceil$ where

$$\hat{N} = \arg_{N}\left\{N\phi - \frac{R}{M} = \frac{Q^{-1}(\theta)\phi}{\sqrt{MTK}}\right\} \Rightarrow \hat{N} = \frac{R}{M\phi} + \frac{Q^{-1}(\theta)}{\sqrt{MTK}}. \quad (27)$$

In (25), (f) is obtained by using the approximation $\log(1+u) \simeq \log(u)$ for large u's and variable transform $u = \frac{N_{\rm r}\phi}{N_{\rm t}}$. Also, $W(x)$ denotes the Lambert W function defined as $ye^y = x \Rightarrow y = W(x)$ [57]. Note that the Lambert W function has an efficient implementation in MATLAB and MATHEMATICA.

For Case 4, we consider two scenarios and use the following approximations.

Case 4 with $K > 1$: Then, $\hat{N}_{\rm r} = \left\lceil\hat{N}\right\rceil, \hat{N}_{\rm t} = \left\lceil K\hat{N}\right\rceil$ and

$$\hat{N} = \arg_{N}\left\{N\log\left(\frac{\phi}{KN}\right) + N\left(\sum_{i=1}^{(K-1)N}\frac{1}{i} - \gamma\right) + \sum_{i=1}^{N-1}\frac{i}{KN-i} - \frac{R}{M}\right.$$
$$\left. = \frac{Q^{-1}(\theta)}{\sqrt{MT}}\sqrt{\sum_{i=1}^{N-1}\frac{i}{((K-1)N+i)^2} + N\left(\frac{\pi^2}{6} - \sum_{i=1}^{KN-1}\frac{1}{i^2}\right)}\right\}$$
$$\overset{(g)}{\simeq} \arg_{N}\left\{N\log\left(\frac{\phi}{KN}\right) + N\left(\log((K-1)N) - \gamma\right)\right.$$
$$\left. + 2 - N + KN\log\left(\frac{KN-1}{(K-1)N+1}\right) - \frac{R}{M} = \frac{Q^{-1}(\theta)}{\sqrt{MT}}\sqrt{\Delta}\right\}$$
$$\overset{(h)}{\simeq} \arg_{N}\left\{N\left(\log(\phi) - \gamma - 1 + (K-1)\log\left(\frac{K}{K-1}\right)\right) - \frac{R}{M}\right.$$
$$\left. = \frac{Q^{-1}(\theta)}{\sqrt{MT}}\sqrt{\log\left(\frac{K}{K-1}\right)}\right\}$$
$$\Rightarrow \hat{N} = \frac{\frac{R}{M} + \frac{Q^{-1}(\theta)}{\sqrt{MT}}\sqrt{\log\left(\frac{K}{K-1}\right)}}{\log(\phi) - \gamma - 1 + (K-1)\log\left(\frac{K}{K-1}\right)},$$
$$\Delta \doteq \frac{(K-1)N(2-N)}{(KN-N+1)(KN-1)} + \log\left(\frac{KN-1}{(K-1)N+1}\right) + N\left(\frac{\pi^2}{6} - \sum_{i=1}^{KN-1}\frac{1}{i^2}\right). \quad (28)$$

Here, (g) is obtained by implementing the Riemann integral approximation $\sum_{i=1}^{n} f(i) \simeq \int_1^n f(x)\mathrm{d}x$ in the first three summation terms. Then, (h) follows from some manipulations, the fact that N is assumed large, and $N(\frac{\pi^2}{6} - \sum_{i=1}^{KN}\frac{1}{i^2}) \to \frac{1}{K}$ for large N's.

Case 4 with $K<1$: Then, $\hat{N}_{\rm r}=\left\lceil \hat{N}\right\rceil, \hat{N}_{\rm t}=\left\lceil K\hat{N}\right\rceil$ and

$$\hat{N}=\underset{N}{\arg}\Bigg\{KN\log\left(\frac{\phi}{KN}\right)+KN\left(\sum_{i=1}^{(1-K)N}\frac{1}{i}-\gamma\right)+\sum_{i=1}^{KN-1}\frac{i}{N-i}-\frac{R}{M}=\frac{Q^{-1}(\theta)}{\sqrt{MT}}\sqrt{\sum_{i=1}^{KN-1}\frac{i}{((1-K)N+i)^2}+KN\left(\frac{\pi^2}{6}-\sum_{i=1}^{N-1}\frac{1}{i^2}\right)}\Bigg\}$$
$$\overset{(g)}{\simeq}\underset{N}{\arg}\Bigg\{KN\log\left(\frac{\phi}{KN}\right)+KN\left(\log((1-K)N)-\gamma\right)+2-KN+N\log\left(\frac{N-1}{(1-K)N+1}\right)-\frac{R}{M}=\frac{Q^{-1}(\theta)}{\sqrt{MT}}\sqrt{\Upsilon}\Bigg\}$$
$$\overset{(h)}{\simeq}\underset{N}{\arg}\Bigg\{NK\Bigg(\log(\phi)-\gamma-1-\log(K)+\left(\frac{K-1}{K}\right)\log(1-K)\Bigg)-\frac{R}{M}=\frac{Q^{-1}(\theta)}{\sqrt{MT}}\sqrt{-\log(1-K)}\Bigg\}$$
$$\Rightarrow\hat{N}=\frac{\frac{R}{M}+\frac{Q^{-1}(\theta)}{\sqrt{MT}}\sqrt{-\log(1-K)}}{K\left(\log(\phi)-\gamma-1-\log(K)+(\frac{K-1}{K})\log(1-K)\right)},$$
$$\Upsilon\doteq\frac{(1-K)N(2-NK)}{(N-NK+1)(N-1)}+\log\left(\frac{N-1}{(1-K)N+1}\right)+NK\left(\frac{\pi^2}{6}-\sum_{i=1}^{N-1}\frac{1}{i^2}\right),\tag{29}$$

where (g) and (h) are obtained with the same procedure as in (28)[6]. Finally, note that with the same arguments as in (24), the optimization problem (5) is rephrased as

$$\{\hat{N}_{\rm t},\hat{N}_{\rm r}\}^{\text{Slow-fading}}=\underset{N_{\rm t},N_{\rm r}}{\arg\min}\left\{\Pr(\text{Outage})^{\text{Slow-Fading}}\leq\theta\right\}=\underset{N_{\rm t},N_{\rm r}}{\arg}\left\{\frac{\mu-\frac{R}{M}}{\sigma}=\frac{Q^{-1}(\theta)}{\sqrt{M}}\right\}\tag{31}$$

and

$$\{\hat{N}_{\rm t},\hat{N}_{\rm r}\}^{\text{Quasi-static}}=\underset{N_{\rm t},N_{\rm r}}{\arg\min}\left\{\Pr(\text{Outage})^{\text{Quasi-static}}\leq\theta\right\}=\underset{N_{\rm t},N_{\rm r}}{\arg}\left\{\frac{\mu-\frac{R}{M}}{\sigma}=Q^{-1}(\theta)\right\},\tag{32}$$

in slow-fading and quasi-static conditions, respectively. Therefore, as stated in the theorem, with slow-fading and quasi-static channel the required numbers of the transmit and/or receive antennas are determined by (10) while the term $\frac{Q^{-1}(\theta)}{\sqrt{MT}}$ is replaced by $\frac{Q^{-1}(\theta)}{\sqrt{M}}$ and $Q^{-1}(\theta)$, respectively.

[6]We can follow the same procedure as in (28)-(29) to write

$$\hat{N}=\underset{N}{\arg}\left\{N(\log(\phi)-\gamma-1)-\frac{R}{M}=\frac{Q^{-1}(\theta)}{\sqrt{MT}}\sqrt{\log(N-1)+1}\right\},\tag{30}$$

in the cases with $K=1$ which can be solved numerically via, e.g., "'fsolve" function of MATLAB or by different approximation schemes. However, for simplicity and because it is a special condition, we do not consider $K=1$ as a separate case.

Appendix B
Proof of Theorem 2

With given initial transmission rate R and SNR ϕ, we use the approximation

$$Q(x)\simeq\frac{e^{-\frac{x^2}{2}}}{2},x\geq0,\tag{33}$$

for large x's and (7) to rewrite the normalized outage factor (12) as

$$\Gamma=\frac{c\left(\mu-\frac{R}{M}\right)^2}{2N_{\rm t}N_{\rm r}\sigma^2},c=\begin{cases}MT, & \text{Fast-fading}\\ M, & \text{Slow-fading}\\ 1, & \text{Quasi-static.}\end{cases}\tag{34}$$

Then, from (8), the normalized outage factor in different cases is found as

$$\Gamma=\begin{cases}\frac{c}{2N_{\rm t}N_{\rm r}}\frac{\left(N_{\rm t}\log\left(1+\frac{N_{\rm r}\phi}{N_{\rm t}}\right)-\frac{R}{M}\right)^2}{\frac{N_{\rm t}}{N_{\rm r}}}\\ \quad=\frac{c}{2}\left(\log\left(1+\frac{N_{\rm r}\phi}{N_{\rm t}}\right)-\frac{R}{MN_{\rm t}}\right)^2 & \text{if Case 1}\\ \frac{c}{2N_{\rm t}N_{\rm r}}\frac{\left(N_{\rm r}\log(1+\phi)-\frac{R}{M}\right)^2N_{\rm t}(1+\phi)^2}{N_{\rm r}\phi^2}\\ \quad=\frac{c}{2}\frac{(1+\phi)^2}{\phi^2}\left(\log(1+\phi)-\frac{R}{MN_{\rm r}}\right)^2 & \text{if Case 2}\\ \frac{c}{2KN^2}\frac{\left(N\phi-\frac{R}{M}\right)^2}{\frac{\phi^2}{K}}=\frac{c}{2} & \text{if Case 3}\\ \frac{c}{2K}\alpha, & \text{if Case 4}\end{cases}$$
$$\alpha=\begin{cases}\frac{\left(\log(\phi)+(K-1)\log\left(\frac{K}{K-1}\right)-\gamma-1\right)^2}{\log\left(\frac{K}{K-1}\right)} & \text{if } K>1\\ \frac{K^2\left(\log(\phi)+\frac{K-1}{K}\log(1-K)-\log(K)-\gamma-1\right)^2}{-\log(1-K)} & \text{if } K<1,\end{cases}$$
$$c=\begin{cases}MT, & \text{Fast-fading}\\ M, & \text{Slow-fading}\\ 1, & \text{Quasi-static,}\end{cases}\tag{35}$$

where α is found by following the same approach as in (28)-(29). Finally, note that to use (33) the initial rate and the SNR should be such that $\mu\geq\frac{R}{M}$ for the considered number of antennas. Otherwise, the outage probability converges to 1 and $\Gamma\to0$.

Appendix C
Proof of Theorem 3

As the first order approximation, all retransmission rounds are used at low SNRs. Thus, the power constraint (17.ii) is simplified to $\frac{\sum_{i=1}^{M}\phi_i}{M}=\phi$. On the other hand, from (15), we have

$$\underset{N_{\rm t},N_{\rm r}}{\arg\min}\left\{\Pr(\text{Outage})\leq\theta\right\}\equiv\underset{N_{\rm t},N_{\rm r}}{\arg\min}\left\{\frac{\bar{\mu}_{(M)}-\frac{R}{M}}{\bar{\sigma}_{(M)}}\leq Q^{-1}(\theta)\right\},\tag{36}$$

where using (8) and the approximation $\log(1+x)\simeq x$ for small x's, the set of means and variances $\left(\mu_{(M)},\bar{\sigma}^2_{(M)}\right)$ are given by $\left(\frac{N_{\rm r}\sum_{i=1}^{M}\phi_i}{M},\frac{N_{\rm t}}{N_{\rm r}TM^2}\right)$, $\left(\frac{N_{\rm r}\sum_{i=1}^{M}\phi_i}{M},\frac{N_{\rm r}\sum_{i=1}^{M}\phi_i^2}{N_{\rm t}TM^2}\right)$ and $\left(\frac{N_{\rm r}\sum_{i=1}^{M}\phi_i}{M},\frac{N_{\rm r}\sum_{i=1}^{M}\phi_i^2}{N_{\rm t}TM^2}\right)$ in Cases 1-3, respectively. In this way, for all Cases 1-3, the optimal power allocation, in terms of (17), tends towards $\phi_i=\phi_j,\forall i,j$, at low SNRs. This is because, replacing $\left(\mu_{(M)},\bar{\sigma}^2_{(M)}\right)$ into (36) for different cases,

both the objective function and the constraint of (17) are symmetric functions of $\phi_i, \forall i$, i.e., the power terms $\phi_i, \forall i$, are interchangeable in (17), at low SNRs.

REFERENCES

[1] B. Gammage, D. C. Plummer, E. Thompson, L. Fiering, H. LeHong, F. Karamouzis, C. Da Rold, K. Collins, W. Clark, N. Jones, C. Smulders, M. Escherich, M. Reynolds, and M. Basso, "Gartner's top predictions for IT organizations and users, 2010 and beyond: A new balance," Gartner Report, Dec. 2009.

[2] N. Bhushan, J. Li, D. Malladi, R. Gilmore, D. Brenner, A. Damnjanovic, R. Sukhavasi, C. Patel, and S. Geirhofer, "Network densification: The dominant theme for wireless evolution into 5G," *IEEE Commun. Mag.*, vol. 52, no. 2, pp. 82–89, Feb. 2014.

[3] T. S. Rappaport, S. Sun, R. Mayzus, H. Zhao, Y. Azar, K. Wang, G. N. Wong, J. K. Schulz, M. Samimi, and F. Gutierrez, "Millimeter wave mobile communications for 5G cellular: It will work!" *IEEE Access*, vol. 1, pp. 335–349, May 2013.

[4] Z. Pi and F. Khan, "An introduction to millimeter-wave mobile broadband systems," *IEEE Commun. Mag.*, vol. 49, no. 6, pp. 101–107, June 2011.

[5] B. Makki and T. Eriksson, "On hybrid ARQ and quantized CSI feedback schemes in quasi-static fading channels," *IEEE Trans. Commun.*, vol. 60, no. 4, pp. 986–997, April 2012.

[6] G. Caire and D. Tuninetti, "The throughput of hybrid-ARQ protocols for the Gaussian collision channel," *IEEE Trans. Inf. Theory*, vol. 47, no. 5, pp. 1971–1988, July 2001.

[7] P. Wu and N. Jindal, "Performance of hybrid-ARQ in block-fading channels: A fixed outage probability analysis," *IEEE Trans. Commun.*, vol. 58, no. 4, pp. 1129–1141, April 2010.

[8] T. V. K. Chaitanya and E. G. Larsson, "Optimal power allocation for hybrid ARQ with chase combining in i.i.d. Rayleigh fading channels," *IEEE Trans. Commun.*, vol. 61, no. 5, pp. 1835–1846, May 2013.

[9] H. El Gamal, G. Caire, and M. O. Damen, "The MIMO ARQ channel: Diversity-multiplexing-delay tradeoff," *IEEE Trans. Inf. Theory*, vol. 52, no. 8, pp. 3601–3621, Aug. 2006.

[10] A. Chuang, et. al, "Optimal throughput-diversity-delay tradeoff in MIMO ARQ block-fading channels," *IEEE Trans. Inf. Theory*, vol. 54, no. 9, pp. 3968–3986, Sept. 2008.

[11] H. Liu, L. Razoumov, N. Mandayam, and P. Spasojević, "An optimal power allocation scheme for the STC hybrid-ARQ over energy limited networks," *IEEE Trans. Wireless Commun.*, vol. 8, no. 12, pp. 5718–5722, Dec. 2009.

[12] K. D. Nguyen, L. K. Rasmussen, A. Guillén i Fábregas, and N. Letzepis, "MIMO ARQ with multibit feedback: Outage analysis," *IEEE Trans. Inf. Theory*, vol. 58, no. 2, pp. 765–779, Feb. 2012.

[13] B. Makki, T. Svensson, T. Eriksson, and M.-S. Alouini, "Adaptive space-time coding using ARQ," *IEEE Trans. Veh. Technol.*, vol. 64, no. 9, pp. 4331–4337, Sept. 2015.

[14] B. Makki and T. Eriksson, "On the performance of MIMO-ARQ systems with channel state information at the receiver," *IEEE Trans. Commun.*, vol. 62, no. 5, pp. 1588–1603, May 2014.

[15] K. Zheng, H. Long, L. Wang, and W. Wang, "Linear space-time precoder with hybrid ARQ transmission," in *Proc. IEEE GLOBECOM'2007*, Washington, DC, USA, Nov. 2007, pp. 3543–3547.

[16] H. Huang and Z. Ding, "Ergodic capacity maximizing MIMO ARQ precoder design based on channel mean information," in *Proc. IEEE ITAW'2008*, San Diego, CA, USA, Feb. 2008, pp. 58–62.

[17] K. Zheng, H. Long, L. Wang, W. Wang, and Y. I. Kim, "Design and performance of space-time precoder with hybrid ARQ transmission," *IEEE Trans. Veh. Technol.*, vol. 58, no. 4, pp. 1816–1822, May 2009.

[18] C. Shen and M. P. Fitz, "Hybrid ARQ in multiple-antenna slow fading channels: Performance limits and optimal linear dispersion code design," *IEEE Trans. Inf. Theory*, vol. 57, no. 9, pp. 5863–5883, Sept. 2011.

[19] Y. Xie and A. J. Goldsmith, "Diversity-multiplexing-delay tradeoffs in MIMO multihop networks with ARQ," in *Proc. IEEE ISIT'2010*, Austin, TX, USA, June 2010, pp. 2208–2212.

[20] P. Hesami and J. N. Laneman, "Low-complexity incremental use of multiple transmitters in wireless communication systems," in *Proc. IEEE Allerton'2011*, Monticello, IL, USA, Sept. 2011, pp. 1613–1618.

[21] T. L. Marzetta, "How much training is required for multiuser MIMO?" in *Proc. IEEE Asilomar'2006*, Pacific Grove, CA, USA, Oct. 2006, pp. 359–363.

[22] ——, "Noncooperative cellular wireless with unlimited numbers of base station antennas," *IEEE Trans. Wireless Commun.*, vol. 9, no. 11, pp. 3590–3600, Nov. 2010.

[23] H. Q. Ngo, T. L. Marzetta, and E. G. Larsson, "Analysis of the pilot contamination effect in very large multicell multiuser MIMO systems for physical channel models," in *Proc. IEEE ICASSP'2011*, Prague, Czech Republic, May 2011, pp. 3464–3467.

[24] J. Jose, A. Ashikhmin, T. L. Marzetta, and S. Vishwanath, "Pilot contamination problem in multi-cell TDD systems," in *Proc. IEEE ISIT'2009*, Soul, South Korea, June 2009, pp. 2184–2188.

[25] K. Appaiah, A. Ashikhmin, and T. L. Marzetta, "Pilot contamination reduction in multi-user TDD systems," in *Proc. IEEE ICC'2010*, Cape Town, South Africa, May 2010, pp. 1–5.

[26] J. Jose, A. Ashikhmin, T. L. Marzetta, and S. Vishwanath, "Pilot contamination and precoding in multi-cell TDD systems," *IEEE Trans. Wireless Commun.*, vol. 10, no. 8, pp. 2640–2651, Aug. 2011.

[27] Z. Xiang, M. Tao, and X. Wang, "Massive MIMO multicasting in noncooperative cellular networks," *IEEE J. Sel. Areas Commun.*, vol. 32, no. 6, pp. 1180–1193, June 2014.

[28] B. Gopalakrishnan and N. Jindal, "An analysis of pilot contamination on multi-user MIMO cellular systems with many antennas," in *Proc. IEEE SPAWC'2011*, San Francisco, CA, USA, June 2011, pp. 381–385.

[29] J. Hoydis, S. ten Brink, and M. Debbah, "Massive MIMO in the UL/DL of cellular networks: How many antennas do we need?" *IEEE J. Sel. Areas Commun.*, vol. 31, no. 2, pp. 160–171, Feb. 2013.

[30] J. Choi, D. J. Love, and P. Bidigare, "Downlink training techniques for FDD massive MIMO systems: Open-loop and closed-loop training with memory," *IEEE J. Sel. Topics Signal Process.*, vol. 8, no. 5, pp. 802–814, Oct. 2014.

[31] X. Rao and V. K. N. Lau, "Distributed compressive CSIT estimation and feedback for FDD multi-user massive MIMO systems," *IEEE Trans. Signal Process*, vol. 62, no. 12, pp. 3261–3271, June 2014.

[32] J. Choi, Z. Chance, D. J. Love, and U. Madhow, "Noncoherent trellis coded quantization: A practical limited feedback technique for massive MIMO systems," *IEEE Trans. Commun.*, vol. 61, no. 12, pp. 5016–5029, Dec. 2013.

[33] H. Q. Ngo, E. G. Larsson, and T. L. Marzettat, "Uplink power efficiency of multiuser MIMO with very large antenna arrays," in *Proc. IEEE Allerton'2011*, Monticello, IL, USA, Sept. 2011, pp. 1272–1279.

[34] H. Huh, G. Caire, H. C. Papadopoulos, and S. A. Ramprashad, "Achieving massive MIMO spectral efficiency with a not-so-large number of antennas," *IEEE Trans. Wireless Commun.*, vol. 11, no. 9, pp. 3226–3239, Sept. 2012.

[35] S. Wagner, R. Couillet, M. Debbah, and D. T. M. Slock, "Large system analysis of linear precoding in correlated MISO broadcast channels under limited feedback," *IEEE Trans. Inf. Theory*, vol. 58, no. 7, pp. 4509–4537, July 2012.

[36] E. Larsson, O. Edfors, F. Tufvesson, and T. Marzetta, "Massive MIMO for next generation wireless systems," *IEEE Commun. Mag.*, vol. 52, no. 2, pp. 186–195, Feb. 2014.

[37] L. Lu, G. Y. Li, A. L. Swindlehurst, A. Ashikhmin, and R. Zhang, "An overview of massive MIMO: Benefits and challenges," *IEEE J. Sel. Topics Signal Process.*, vol. 8, no. 5, pp. 742–758, Oct. 2014.

[38] F. Rusek, D. Persson, B. K. Lau, E. G. Larsson, T. L. Marzetta, O. Edfors, and F. Tufvesson, "Scaling up MIMO: Opportunities and challenges with very large arrays," *IEEE Signal Process. Mag.*, vol. 30, no. 1, pp. 40–60, Jan. 2013.

[39] B. M. Hochwald, T. L. Marzetta, and V. Tarokh, "Multiple-antenna channel hardening and its implications for rate feedback and scheduling," *IEEE Trans. Inf. Theory*, vol. 50, no. 9, pp. 1893–1909, Sept. 2004.

[40] Y. Polyanskiy, H. V. Poor, and S. Verdu, "Channel coding rate in the finite blocklength regime," *IEEE Trans. Inf. Theory*, vol. 56, no. 5, pp. 2307–2359, May 2010.

[41] W. Yang, G. Durisi, T. Koch, and Y. Polyanskiy, "Quasi-static multiple-antenna fading channels at finite blocklength," *IEEE Trans. Inf. Theory*, vol. 60, no. 7, pp. 4232–4265, July 2014.

[42] mmMagic Deliverable D1.1, "Use case characterization, KPIs and preferred suitable frequency ranges for future 5G systems between 6 GHz and 100 GHz," Nov. 2015, available at: https://5g-mmmagic.eu/results/.

[43] Ericsson AB, "Delivering high-capacity and cost-efficient backhaul for broadband networks today and in the future," Sept. 2015, available at: http://www.ericsson.com/res/docs/2015/microwave-2020-report.pdf.

[44] B. Makki and T. Eriksson, "On the average rate of quasi-static fading channels with ARQ and CSI feedback," *IEEE Commun. Lett.*, vol. 14, no. 9, pp. 806–808, Sept. 2010.

[45] ——, "Feedback subsampling in temporally-correlated slowly-fading channels using quantized CSI," *IEEE Trans. Commun.*, vol. 61, no. 6, pp. 2282–2294, June 2013.

[46] T. M. Cover and J. A. Thomas, *Elements of Information Theory*. New York: Wiley Interscience, 1992.

[47] A. El Gamal and Y.-H. Kim, "Lecture notes on network information theory," 2010, [Online]. Available at *http://arxiv.org/abs/1001.3404v4/*.
[48] E. Bjornemo, "Energy constrained wireless sensor networks: communication principles and sensing aspects," Ph.D. dissertation, Uppsala University, Uppsala, Sweden, 2009.
[49] S. Mikami, T. Takeuchi, H. Kawaguchi, C. Ohta, and M. Yoshimoto, "An efficiency degradation model of power amplifier and the impact against transmission power control for wireless sensor networks," in *Proc. IEEE RWS'2007*, Long Beach, CA, USA, Jan. 2007, pp. 447–450.
[50] D. Persson, T. Eriksson, and E. G. Larsson, "Amplifier-aware multiple-input single-output capacity," *IEEE Trans. Commun.*, vol. 62, no. 3, pp. 913–919, March 2014.
[51] B. Makki, A. Graell i Amat, and T. Eriksson, "On noisy ARQ in block-fading channels," *IEEE Trans. Veh. Technol.*, vol. 63, no. 2, pp. 731–746, Feb. 2014.
[52] B. Makki, T. Svensson, and M. Zorzi, "Finite block-length analysis of the incremental redundancy HARQ," *IEEE Wireless Commun. Lett.*, vol. 3, no. 5, pp. 529–532, Oct. 2014.
[53] B. E. Godana and T. Ekman, "Parametrization based limited feedback design for correlated MIMO channels using new statistical models," *IEEE Trans. Wireless Commun.*, vol. 12, no. 10, pp. 5172–5184, Oct. 2013.
[54] I. M. Kim, "Exact BER analysis of OSTBCs in spatially correlated MIMO channels," *IEEE Trans. Commun.*, vol. 54, no. 8, pp. 1365–1373, Aug. 2006.
[55] A. L. Moustakas, S. H. Simon, and A. M. Sengupta, "MIMO capacity through correlated channels in the presence of correlated interferers and noise: A (not so) large N analysis," *IEEE Trans. Inf. Theory*, vol. 49, no. 10, pp. 2545–2561, Oct. 2003.
[56] K. S. Ahn and R. W. Heath, "Performance analysis of maximum ratio combining with imperfect channel estimation in the presence of cochannel interferences," *IEEE Trans. Wireless Commun.*, vol. 8, no. 3, pp. 1080–1085, Mar. 2009.
[57] R. M. Corless, G. H. Gonnet, D. E. G. Hare, D. J. Jeffrey, and D. E. Knuth, "On the Lambert W function," *Advances in Computational Mathematics*, vol. 5, pp. 329–359, 1996.

Behrooz Makki was born in Tehran, Iran. He received the B.Sc. degree in Electrical Engineering from Sharif University of Technology, Tehran, Iran, and the M.Sc. degree in Bioelectric Engineering from Amirkabir University of Technology, Tehran, Iran, respectively. Behrooz received his PhD degree in Communication Engineering from Chalmers University of Technology, Gothenburg, Sweden. Since 2013, he is working as a Postdoc at Chalmers University. Behrooz is the recipient of VR Research Link grant, Sweden, 2014, and the Ericsson's Research grant, Sweden, 2013, 2014 and 2015. Also, he is a member of European Commission 5G project "mm-Wave based Mobile Radio Access Network for 5G Integrated Communications." His current research interests include partial channel state information (CSI) feedback, hybrid automatic repeat request, Green communication, millimeter wave communication, free-space optical communication and finite block-length analysis.

TOMMY SVENSSON [S'98, M'03, SM'10] is Associate Professor in Communication Systems at Chalmers University of Technology in Gothenburg, Sweden, where he is leading the research on air interface and wireless backhaul networking technologies for future wireless systems. He received a Ph.D. in Information theory from Chalmers in 2003, and he has worked at Ericsson AB with core networks, radio access networks, and microwave transmission products. He was involved in the European WINNER and ARTIST4G projects that made important contributions to the 3GPP LTE standards, the recently finished EU FP7 METIS 5G project and is currently involved in the EU H2020 5GPPP mmMAGIC project targeting mm-wave solutions for 5G. His main research interests are in design and analysis of physical layer algorithms, multiple access, resource allocation, cooperative systems, moving networks and satellite networks. He has co-authored three books and more than 120 journal and conference papers. He is Chairman of the IEEE Sweden joint Vehicular Technology/Communications/Information Theory Societies chapter, and coordinator of the Communication Engineering Master's Program at Chalmers.

Thomas Eriksson received the Ph.D. degree in Information Theory in 1996, from Chalmers University of Technology, Gothenburg, Sweden. From 1990 to 1996, he was at Chalmers. In 1997 and 1998, he was at AT&T Labs - Research in Murray Hill, NJ, USA, and in 1998 and 1999 he was at Ericsson Radio Systems AB, Kista, Sweden. Since 1999, he has been at Chalmers University, where he is a professor in communication systems. Further, he was a guest professor at Yonsei University, S. Korea, in 2003-2004. He has authored and co-authored more than 200 journal and conference papers, and is the inventor of 7 patents.

Prof. Ericsson is leading the research efforts on hardware-constrained communications at Chalmers. His research interests include communication, data compression, and modeling and compensation of non-ideal hardware components (e.g. amplifiers, oscillators, modulators in communication transmitters and receivers, including massive MIMO). He is currently vice head of the department of Signals & Systems at Chalmers, with responsibility for undergraduate and master education.

Mohamed-Slim Alouini (S'94, M'98, SM'03, F'09) was born in Tunis, Tunisia. He received the Ph.D. degree in Electrical Engineering from the California Institute of Technology (Caltech), Pasadena, CA, USA, in 1998. He served as a faculty member in the University of Minnesota, Minneapolis, MN, USA, then in the Texas A&M University at Qatar, Education City, Doha, Qatar before joining King Abdullah University of Science and Technology (KAUST), Thuwal, Makkah Province, Saudi Arabia as a Professor of Electrical Engineering in 2009. His current research interests include the modeling, design, and performance analysis of wireless communication systems.